# Recent progress in the design fabrication of metal-organic frameworks-based nanozymes and their applications to sensing and cancer therapy

Xianlong Zhang[a], Guoliang Li[a,d,*], Di Wu[e], Xiuling Li[f], Na Hu[b], Jian Chen[a], Guang Chen[d], Yongning Wu[c]

[a] School of Food and Biological Engineering, Shaanxi University of Science and Technology, Xi'an, 710021, China
[b] Key Laboratory of Tibetan Medicine Research, Qinghai Provincial Key Laboratory of Tibetan Medicine Research, Northwest Institute of Plateau Biology, Chinese Academy of Sciences, Xining, 810001, China
[c] Key Laboratories of Chemical Safety and Health, China National Center for Food Safety Risk Assessment, Beijing, 100050, China
[d] Key Laboratory of Life-Organic Analysis of Shandong Province, Qufu Normal University, Qufu, 273165, China
[e] Yangtze Delta Region Institute of Tsinghua University, Zhejiang, 314006, China
[f] Beijing Advanced Innovation Center for Food Nutrition and Human Health, Beijing Technology and Business University, Beijing, 100048, China

## ARTICLE INFO

## ABSTRACT

The nanomaterials with enzyme-like catalytic activity, named as nanozymes, have aroused wide research interest owing to their striking merits. Metal-organic frameworks (MOFs) have showed great prospect in the construction of novel nanozymes. In this review, firstly, we summarize the most recent contributions in the design construction of the MOFs-based nanozymes. Then, we concentrate our attention on their applications in the fields of sensing and cancer therapies. According to the design strategies, we categorized MOFs-based nanozymes into four classes for review (i.e. pristine MOFs, MOFs with modification, MOFs-based nanocomposites, and MOF derivatives). Meanwhile, the emerging and fascinating 2D MOFs-based nanozymes were also reviewed. A variety of novel applications are also discussed, including nanozymes catalytic mediated signal amplification in sensing applications (e.g. colorimetric sensing, fluorescent sensing, chemiluminescent sensing, electrochemical sensing, and surface-enhanced Raman scattering (SERS)), and nanozymes catalytic mediated cancer therapy (i.e. cancer-starvation therapy, enhancing photodynamic therapy, and cancer-starvation and PDT synergistic therapy). At the end of the article, future opportunities and challenges in this promising research area are tentatively proposed.

## 1. Introduction

Natural enzymes are very vital biological macromolecules for life, which can efficiently and selectively catalyze a variety of biochemical reactions. They play an important role in many fields, including biosensing(Chen et al., 2018h; Pham et al., 2018), chemical sensing (Ma et al., 2016), biofuels(Tan and Sato, 2017), food industry(Homaei et al., 2013), disease diagnosis and treatment(Chen et al., 2017c; Dinda et al., 2018), etc(Wu et al., 2017a). However, their high manufacturing costs, production complexity, instability, and harsh catalytic conditions limit their wide applications(Gao and Yan, 2016). With the rapid progress and development of nanotechnology, nanomaterials with enzyme-like catalytic activity have attracted the attention of researchers due to their good stability and simple production, which also have been applied for multiple fields(Huang et al., 2019b; Huo et al., 2019; Wang et al., 2018d; Wei and Wang, 2013; Wu et al., 2019), such as environmental protection (He et al., 2018a; Ma et al., 2019), disease diagnosis and treatment(Wang et al., 2018d; Yin et al., 2019), and sensing (Farka et al., 2018; Li et al., 2018a).

In the past twenty years, MOFs as a class of porous crystalline materials have attracted widespread interests and achieved a rapid and remarkable development. MOFs possess the periodic network structures made by self-assembly of organic linkers (e.g. carboxylate ligands and other negatively charged ligands) and inorganic metal-containing nodes (e.g. metal ions and clusters). MOFs possess many attractive properties such as high surface area and highly tunable pore sizes (generally 0–3 nm, up to 9.8 nm)(Jiao et al., 2018; Yang et al., 2017b), which have been widely applied in multiple fields and still have great potential for further development (Xu et al., 2018; Zhao et al. 2018c, 2018d). MOFs possess active sites with high density and uniform dispersion, and their

---

**Abbreviations**

| | |
|---|---|
| ALP | alkaline phosphatase |
| AFP | alpha-fetoprotein |
| AA | ascorbic acid |
| AUR | Amplex UltraRed |
| AZBTS | 2, 2′-azinobis (3-ethylbenzothizoline-6-sulfonic- acid) |
| BHb | bovine hemoglobin |
| BTC | 1, 3, 5-benzenetricarboxylic acid |
| BPY | 4, 4′-Bipyridine |
| CL | chemiluminescence |
| Cu-MOF | copper (II)-based MOFs |
| Cys | cysteine |
| DTDBA | 2, 2′-Dithiosalicylic acid |
| DA | dopamine |
| GCE | glassy carbon electrode |
| GOx/GOD | glucose oxidase |
| HRTEM | high resolution transmission electron microscopy |
| $H_2DMTDC$ | 3,4-dimethylthieno[2,3-b]thiophene-2,5-dicarboxylic acid |
| $H_2O_2$ | hydrogen peroxide |
| INAzymes | integrated nanozymes |
| MG | malachite green |

| | |
|---|---|
| MOF | metal organic framework |
| MNPs | metal nanoparticles |
| NPs | nanoparticles |
| $NH_2$-BDC | 2-amino-terephthalc acid |
| OPD | o-phenyl-enediamine |
| $O_2$ | oxygen |
| PtNCs | platinum nanoclusters |
| PPi | pyrophosphate |
| Pi | phosphate |
| PDT | photodynamic therapy |
| PB | prussian blue |
| PTT | photothermal therapy |
| SERS | surface-enhanced Raman scattering |
| SDT | sonodynamic therapy |
| ssDNA | single-stranded DNA |
| TH | thiamine |
| TPZ | tirapazamine |
| TMB | 3, 3′, 5, 5′–tetramethylbenzidine |
| UA | uric acid |
| 3D/2D | Three/two-dimensional |
| $^1O_2$ | singlet oxygen |
| 1, 4-BDC | 1,4-benzene-dicarboxylic acid |

porous structure and multiple channels can facilitate small molecule substrates to enter and fully contact with the active sites, which are also beneficial to transport and diffusion of products. In addition, high uniform sizes and pore shapes of MOFs are important to size-selective catalytic reaction, which can effectively control the size of the participating molecules. Therefore, larger molecules can't enter the micro pores to participate in the catalytic reactions (Yang et al., 2017b). By right of the excellent catalytic characteristics, MOFs have been recognized as the promising nanomaterials for the preparation of novel nanozymes and gradually attracted the wide attentions. MOFs have been widely applied in multiple fields, such as biocatalysis(Fu et al., 2018; Jiao et al., 2018), chemicalsensing(Kukkar et al., 2018), biosensing(Li et al., 2019a; Zhou et al., 2018b), and electrochemistry(Liu et al., 2016; Liu and Yin, 2016). However, unsaturated metal centers and unstable activity of MOFs limit their range of applications (Vermoortele et al., 2013; Wang et al., 2011). Recently, MOFs-based nanocomposites can endow the nanozymes with a higher activity and a stronger stability, and make up for the disadvantage of MOFs in some extent, allowing a rapid development stage of MOFs-based nanozymes. Although 3D MOFs based nanozymes have many remarkable advantages, their poor dispersion in aqueous solution often limits the accessibility of the target molecules to active sites (Chen et al., 2018a).

Recently, two-dimensional (2D) MOFs (He et al., 2018b; Ko et al., 2018; Tan et al., 2017b; Zhao et al., 2018c; Zhao et al., 2018e) have joined the family of 2D nanomaterials and gradually entered the visual field of researchers. And 2D MOFs with large lateral size are mechanically flexible, optically transparent, and ultrathin. Furthermore, 2D MOFs possess some unique properties, which originate from their larger surface area, ultrathin thickness, and high surface-to-volume atom ratios (Zhao et al., 2018b). In addition, 2D MOFs have higher catalytic activities due to their ultra-large specific surface area and larger active sites for substrates contact (Song and Hu, 2014; Zhang, 2015). On this basis, 2D MOFs have been also widely applied in catalysis, sensing, gas separation, energy, and so on (Feng et al., 2018; Ye et al., 2018; Zhang et al., 2019; Zhang et al., 2018i; Zhao et al., 2018c). Based on the merits of 2D MOFs, 2D MOFs-based nanozyms have also been successfully developed (Chen et al., 2018a; Zhao et al., 2018b).

In this review, we not only comprehensively summarize the recent research progress on the design construction of 3D MOFs-based nanozymes (Table 1), and their sensing applications and therapeutic

applications, but also first summarize the design fabrication of 2D MOFs-based nanozymes (Table 1) and their applications. Moreover, we summarized the sensing methods constructed via MOFs-based nanozymes catalytic mediated diversified signal amplification and signal output, involving the sensing modes of colorimetric sensing, fluorescent sensing, chemiluminescent sensing, electrochemical sensing, and SERS sensing. Impressively, we also summarize cancer therapy based on the MOFs-based nanozymes catalytic triggered cancer cell apoptosis, including cancer-starvation therapy, enhancing photodynamic therapy (PDT), and cancer-starvation and PDT synergistic therapy. In the end, the challenges and opportunities about the further design and applications of MOFs-based nanozymes are put forward.

## 2. Synthetic strategies of MOFs-based nanozymes

### 2.1. 3D MOFs-based nanozymes

#### 2.1.1. Pristine 3D MOFs

Three-dimensional (3D) MOFs have been intensively studied as functional materials for multiple fields, which are coordination polymers composed of metallic nodes and organic linkers (Chen and Wu, 2018; Kreno et al., 2012; Liang et al., 2018c). The large specific surface area and high porosity, together with abundant active sites and transition metals (e.g. Fe, Cu, Co and Zn) endow MOFs with excellent catalytic ability (Chen and Wu, 2018; Kreno et al., 2012; Liang et al., 2018c). Up to now, a lot of 3D MOFs with enzyme-like catalytic activity have been discovered. MIL-type MOFs have been reported with intrinsic peroxidase-like catalytic activity, including MIL-53, MIL-88, MIL-100, MIL-101 and so on. The peroxidase substrates TMB, AZBTS and OPD can be catalyzed by these MIL-type MOFs and lead to a color reaction with the presence of hydrogen peroxide ($H_2O_2$) (Chen et al., 2017a; Dong et al., 2018; Yi et al., 2016b). For example, Jiang et al. successfully prepared two water-stable Fe (III)-based MOFs with intrinsic peroxidase-like properties by a solvothermal reaction. The as-synthesized MIL-68 and MIL-100 both exhibited peroxidase-like activities and could catalyze the peroxidase substrate TMB to produce a remarkable blue color reaction in the presence of $H_2O_2$(Zhang et al., 2014). Lu et al. successfully synthesized a new porous MOF MIL-53(Fe) through using a simple solvothermal way via using $FeCl_3 \cdot 6H_2O$ and 1, 4-benzenedicarboxylic acid as the precursor. The as-obtained product showed an
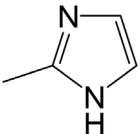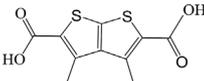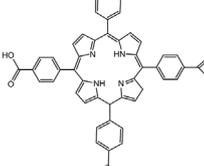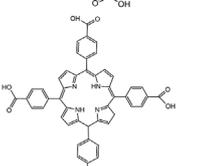
**Table 1**

Summary of 3D/2D MOF-based nanozymes.

The reported 3D MOF-based nanozymes

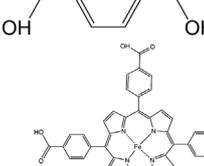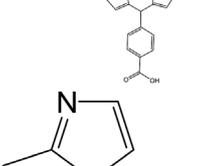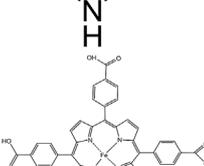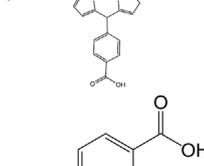| Ligand structure | Ligand abbreviation | Metal | Nanozymes name | Ref. |
|---|---|---|---|---|
|  | 1,4-benzene-dicarboxylic acid (1,4-BDC) | $Fe^{3+}$ | MIL-53(Fe)<br>MIL-53(Fe)<br>MIL-53(Fe)<br>MIL-53(Fe)<br>MIL-68<br>Fe-MIL-88<br>PB/MIL-101(Fe) glycine-MIL-53(Fe)<br>MOF-235/β-cyclodextrin<br>AgNPs/MIL-101 (Fe)<br>$Fe_3O_4$/MIL-101(Fe)<br>$Fe_3O_4$/MIL-101(Fe)<br>PB/MIL-101(Fe) | Ai et al. (2013)<br>Qin et al. (2013)<br>Yi et al. (2016b)<br>Dong et al. (2017a)<br>Zhang et al. (2014)<br>Zhao et al. (2016)<br>Cui et al. (2015b)<br>Dong et al. (2017a)<br>Mao et al. (2018)<br>Jiang et al. (2015)<br>Jiang et al. (2016)<br>Qian Tang et al. (2018)<br>Cui et al. (2015a) |
|  | 2-amino-terephthalc acid (NH₂-BDC) | $Fe^{3+}$<br>$Zr^{4+}$<br>$Cu^{2+}$<br>$Ce^{3+}$<br>$Co^{2+}$<br>$Al^{3+}$ | Fe-MIL-88NH₂<br>NH₂-MIL-88(Fe)<br>PdNPs@Fe-MOFs<br>UiO-66(NH₂)<br>Cu@UiO<br>Cu-MOF<br>AuNPs/Ce-MOFs<br>PtNPs@Co(II)MOFs@ PtNPs<br>Hemin@MOF | (Liu et al., 2013)<br>Dong et al. (2018)<br>Li et al. (2018e)<br>(Hu et al., 2016)<br>Zhao et al. (2018a)<br>Wang et al. (2017)<br>Shen et al. (2016)<br>Yang et al. (2017d)<br>(Qin et al., 2013) |
|  | 1,3,5-benzenetricarboxylic acid (BTC) | $Fe^{3+}$<br>$Zr^{4+}$<br>$Cu^{2+}$ | MIL-100<br>HAP@MIL-100(Fe)<br>$Fe_3O_4$/MIL-100(Fe)<br>$Fe_3O_4$@Au@MIL-100<br>TMBDA-MIL-100(Fe)<br>MOF-808<br>MOF-808F<br>Hemin@HKUST-1<br>HKUST-1 | (Zhang et al., 2014)<br>Chen et al. (2017a)<br>Wu et al. (2017b)<br>Ma et al. (2018)<br>Valekar et al. (2018)<br>Vo et al. (2018)<br>Zheng et al. (2018)<br>Luo et al. (2015)<br>Tan et al. (2015) |
|  | Fumaric acid | $Fe^{3+}$ | Fe-MIL-88A<br>MIL-88 | (Wang et al., 2016c)<br>Gao et al. (2017a) |
|  | 1,4-benzene-dicarboxylic acid (1,4-BDC) | $Cr^{3+}$<br>$Zr^{4+}$ | MIL-101(Cr)@PB<br>AuNPs@MIL-101<br>Cellulase@MOFs<br>UiO-66(NH₂)<br>AgNPs@ ZnMOF | Su et al. (2016)<br>Hu et al. (2017a)<br>(Ahmed et al., 2018)<br>Liu et al. (2018e)<br>Bagheri et al. (2018) |
|  | nucleotide | $Cu^{2+}$ | Gu/GMP | (Liang et al., 2017) |
|  | 4,4′-Bipyridine (BPY) | $Cu^{2+}$ | Cu-MOF<br>RIgG@Cu-MOF | (Wang et al., 2018a)<br>Wang et al. (2018b) |
|  | 2,2′-bipyridine-5,5-dicarboxylic acid | $Zr^{4+}$ | $Cu^{2+}$-NMOF | (Chen et al., 2018f) |
|  | 2,2′-Dithiosalicylic acid (DTDBA) | $Cu^{2+}$ | Cu–MOF | (Menon et al., 2018) |
|  | 1,4-BDC<br>BPY | $Co^{2+}$ | (Co(pbda)(4,4-bpy).2H₂O)ₙ | (Yang et al., 2015) |
| | 2-methylimidazole | $Co^{2+}$ | ZIF-67<br>Co-ZIF-67 | (Qin et al., 2017)<br>Nguyen et al. (2018) |

**Table 1** (*continued*)

The reported 3D MOF-based nanozymes

| Ligand structure | Ligand abbreviation | Metal | Nanozymes name | Ref. |
|---|---|---|---|---|
| | 3,4-dimethylthieno[2,3-b] thiophene-2,5-dicarboxylc acid (H $_2$ DMTDC) | $Ce^{3+}$ | Ce-MOF | (Dalapati et al., 2017) |
| | TCPP | $Zr^{4+}$ | PCN-222<br>PCN-224<br>PCN-224-Pt | (Zhang et al., 2016)<br>Li et al. (2017a)<br>(Zhang et al., 2018j) |
| | TCPP<br>1,4-BDC | $Zr^{4+}$ | UiO-66-TPP-SH | (Kan et al., 2018) |
| | 1,4-BDC<br>TCPP(Fe) | $Zr^{4+}$ | HP-PCN-224(Fe) | (Liu et al., 2018d) |
| | 2-methylimidazole | $Zn^{2+}$ | ZIF-8@BHb<br>ZIF-8/Zn–Al<br>GOx/hemin@ZIF-8 hemin/ZIF-8<br>Au@ZIF-8 | Yin et al. (2016)<br>Hu et al. (2018a)<br>Cheng et al. (2016)<br>Li et al. (2016a)<br>Wang et al. (2016a) |
| | TCPP(Fe) | $Co^{2+}$<br>$Zn^{2+}$<br>$Co^{2+}$<br>$Cu^{2+}$ | Co-TCPP(Fe) MOF<br>AG73@2DM-TCPP(Fe)<br>(M = Zn, Co, Cu) | (Wang et al., 2016b)<br>Cheng et al. (2017) |
| | NH$_2$-BDC | $Cu^{2+}$ | NH$_2$ –Cu-MOF | (Hu et al., 2018b) |
| | BTC | $Cu^{2+}$ | Cu(HBTC)-1/Fe$_3$O$_4$-AuNs | (Tan et al., 2017a) |
| | TCPP(M) | $Cu^{2+}$ | Au NPs/Cu-TCPP(M)<br>(M = Fe, Co) | (Huang et al., 2017b) |
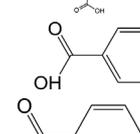
**Table 1** (*continued*)

The reported 3D MOF-based nanozymes

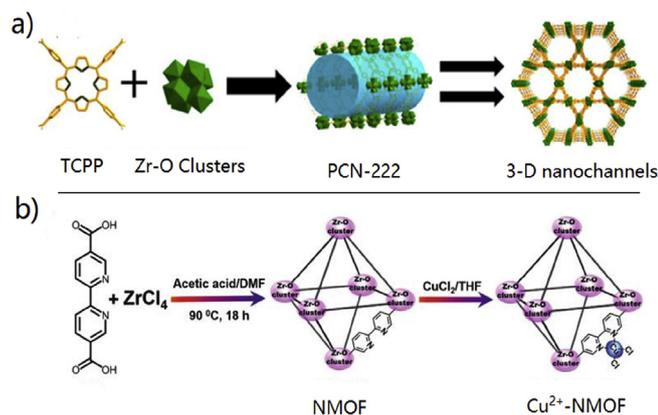| Ligand structure | Ligand abbreviation | Metal | Nanozymes name | Ref. |
|---|---|---|---|---|
| | 1,4-BDC | $Ni^{2+}$ | 2D Ni-MOF nanosheet | (Chen et al., 2018c) |
| | | | Ni-MOF/Ni/NiO | Chen et al. (2018d) |
| | TCPP(Fe) | $Zn^{2+}$ | 2D M-TCPP(Fe) | Qin et al. (2018) |
| | | $Co^{2+}$ | (M = Zn, Co, Cu) | (Chen et al., 2018a) |
| | | $Cu^{2+}$ | PtNPs/Cu-TCPP(Fe) | Liang et al. (2018a) |
| | | $Cu^{2+}$ | GOD@Co-FeMOF | |
| | | $Co^{2+}$ | | |

**Fig. 1.** (a) Schematic illustration for the construction of PCN-222 (Zhang et al., 2016). (b) Synthesis of the $Cu^{2+}$-functionalized $Zr^{4+}$-5,5′-bipyridine carboxylate-bridged metal-organic framework nanoparticles (NMOFs)(Chen et al., 2018f).

intrinsic peroxidase-like activity and could catalyze the oxidation of the peroxidase substrate TMB to generate a blue colored product with the presence of $H_2O_2$(Lu et al., 2015). Wang's group successfully fabricated an ion-based MOF material (Fe-MIL-88A) with high peroxidase-like catalytic activity and could catalyze the peroxidase substrate TMB to produce a blue color. Interestingly, the peroxidase-like catalytic activity of Fe-MIL-88A could be strongly inhibited with the presence of target biomolecule (thrombin) and corresponding aptamer because of the introduction of aptamer and thrombin mixture which could wrap around Fe-MIL-88A. Due to the inhibition of the peroxidase-like catalytic activity, the produced blue color disappeared. On this basis, a novel label-free colorimetric sensing strategy was successfully developed for the detection of biomolecule (e.g. thrombin). With this method, thrombin could be detected with a low detection limit (LOD) of 10 nM through naked eyes (Wang et al., 2016c). Similarly, the Cu-MOFs have been verified to possess enzyme-like catalytic activity (Chen et al., 2018f; Menon et al., 2018; Wang et al. 2018a, 2018b). Li et al. successfully fabricated Cu-MOF with the microporous network and typical octahedral crystals, which exhibited high intrinsic protease-like activity and good stability for catalyzing the proteins at aqueous solution (Li et al., 2014). Furthermore, Wang and co-workers reported Cu-MOFs nanoparticles with peroxidase-like activity, which were fabricated by using

$Cu(NO_3)_2$ and 2-aminoterephthalic acid, and could catalyze the peroxidase substrate TMB to produce a yellow chromogenic reaction in the presence of $H_2O_2$(Wang et al., 2017). Shortly afterwards, Tan's group developed Cu-MOFs, which exhibited horseradish peroxidase-like catalytic activity for detecting the catalytic activity of alkaline phosphatase (ALP) (Wang et al., 2018a). Sheela et al. reported a new Cu-MOF with intrinsic peroxidase-like activity, which was synthesized by solvothermal method and used for sensitive detection of $H_2O_2$ and glucose (Menon et al., 2018). Liu's group successfully synthesized a new Co-MOF with remarkable peroxidase-like activity, (Co(pbda)(4,4-bpy).2$H_2O$)n, which could catalyze $H_2O_2$ to produce ·OH due to its peroxidase-like activity(Yang et al., 2015). A bimetallic MOF (Co/2Fe) was successfully contracted under hydrothermal conditions by Ye and co-workers, which possessed both oxidase-like and peroxidase-like activities. Whether the presence or absence of $H_2O_2$, MOF(Co/2Fe) could both catalyze peroxidase substrate TMB to produce a chromogenic reaction (Yang et al., 2017a). According to previous literature, some Ce-based MOFs with oxidase mimicking activity have been developed successfully. Biswas et al. successfully prepared a cerium-based MOF material by incorporating cerium (IV) ammonium nitrate and 3,4-dimethylthieno[2,3-b]thiophene-2,5-dicarboxylic acid under solvothermal conditions. The developed Ce-MOF possessed an inherent oxidase-like catalytic activity due to the presence of redox-active cerium atoms in the Ce-MOF, which could oxidize TMB or AZBTS without any external oxidizing agents (Dalapati et al., 2017). Recently, another mixed valence state cerium-based MOF (MVC-MOF) was synthesized by Tan and co-workers, which both possessed Ce (III) and Ce (IV) ions due to partial oxidation of cerium (III). The as-prepared MVC-MOF was endowed with a typical oxidase-mimicking activity by Ce (IV), and could oxidize TMB to produce a chromogenic reaction with the presence of oxygen. The ssDNA could inhibit the catalytic activity of the MVC-MOF, because it could bind the MVC-MOF and lead to the active sites of MVC-MOF were shielded, but double-stranded DNA (dsDNA) had negligible influence on the catalytic activity of the MVC-MOF. Based on these characteristics, a novel strategy was developed for the detection of Hg (II)(Wang et al., 2018c). In addition, zirconium-based MOFs had been reported to exhibit enzyme-like catalytic activity. It was worth noting that Zhang's group carried out the research on mimic enzyme activities of zirconium-based porphyrinic MOFs (PCN-222) (Fig. 1a). In this study, the as-synthesized PCN-222 could produce a heterogeneous catalysis as an catalyst in oxygen reduction reaction, which had a great advantage over the enrichment of oxygen molecules

compared to tetrakis(4-carboxyphenyl)porphyrin ligand due to its tunable structures and high porosity(Zhang et al., 2016). In a very recent study, Zheng and co-workers for the first time designed and prepared a novel and stable Zr-based MOF ([Zr$_6$O$_4$($\mu_3$-OH)$_4$(OH)$_6$(H$_2$O)$_6$(BTC)$_2$]·nH$_2$O), named MOF-808, which was synthesized by using hydrochloric acid to treat MOF-808FA, the latter was built by BTC$^{3-}$ linkers and [Zr$_6$O$_4$($\mu_3$-OH)$_4$(FA)$_6$] clusters and formed three-dimensional framework with two types of cages. MOF-808 was verified to exhibit an excellent intrinsic peroxidase-like catalytic activity under acidic, neutral, and alkaline conditions. In the presence of H$_2$O$_2$, the as-prepared MOF-808 was able to catalyze TMB to form blue oxTMB(Zheng et al., 2018).

### 2.1.2. 3D MOFs with modification

Functionalized modifications of MOFs have been known as effective and flexible approaches to introduce the required functionalities into MOF materials, which are usually realized through chemical modifications. Generally speaking, MOFs can be functionalized by their metal nodes and/or organic linkers (Cohen, 2017; Deng et al., 2010). In previous reports, functionalized MOFs have also been widely applied in catalysis. For example, Cui and co-workers successfully synthesized a novel microporous PB/MIL-101(Fe) by modifying Prussian blue (PB) at the exposure metal sites of MIL-101(Fe) in the process of fabrication. It was proved that PB was bound to the surface of MIL-101(Fe) by coordinating vacant Fe$^{3+}$ sites of MIL-101(Fe)s' surface with CN residues on the PB backbone. The as-obtained PB/MIL-101(Fe) exhibited an efficient and excellent peroxidase-like catalytic activity for the reduction of H$_2$O$_2$ and could oxidize the peroxidase substrate TMB, AZBTS and OPD to produce a chromogenic reaction in the presence of H$_2$O$_2$(Cui et al., 2015b). The functional species could also be introduced into MOF through post-synthetic modification way. For example, Chen and co-workers successfully prepared UiO-type MOF nanoparticles (Cu$^{2+}$-NMOFs) (Fig. 1b) using 2,2′-bipyridine-5,5′-dicarboxylic acid as ligands and Zr$^{4+}$ ions as metallic nodes, the bipyridine ligands in Cu$^{2+}$-NMOFs provided uncoordinated chelating centers for the complexation of various metal centers. The developed Cu$^{2+}$-NMOFs possessed peroxidase-like catalytic activity and could catalyze the oxidation of Amplex-Red to produce the fluorescent resorufin by H$_2$O$_2$. Moreover, the

obtained product could catalyze the oxidation of dopamine to generate aminochrome by H$_2$O$_2$ and could produce luminol chemiluminescence with the presence of H$_2$O$_2$(Chen et al., 2018f). As reported by Dong's group, a novel glycine functionalized MIL-53(Fe) (glycine-MIL-53(Fe)) was rationally designed and successfully fabricated through post-synthetic method. The as-prepared glycine-MIL-53(Fe) showed a stronger peroxidase-like activity and smaller K$_m$ for TMB than MIL-53(Fe). In addition, the stability of the glycine-MIL-53(Fe) under both acidic and alkaline conditions exhibited better than that of MIL-53(Fe) due to the presence of amino groups and carboxylic acid in glycine molecular. In the presence of H$_2$O$_2$, the glycine-MIL-53(Fe) could catalyze the oxidation of peroxidase substrate TMB to generate an intensive color change (Dong et al., 2017b). In a recent study, encouraged by the advantages of surface modification of MOFs, Ma's group managed to fabricate a new β-cyclodextrin functionalized MOF-235/β-CD hybrid via a simple method, using β-CD to modify MOF-235 for the first time. It was found that the formation of the MOF-235/β-CD hybrids was ascribed to the coordination interaction between the unsaturated Fe (III) metal ions of MOF-235 and the –OH groups of β-CD. The as-obtained MOF-235/β-CD hybrids showed high catalytic activity for the H$_2$O$_2$-luminol system, and the enhancement of chemiluminescence (CL) intensity was 30-fold more than that of previous H$_2$O$_2$-luminol system (Mao et al., 2018).

### 2.1.3. 3D MOFs-based composites

MOFs possess active sites with high density and uniform dispersion, and their porous structure and multiple channels facilitate substrates to enter and contact with the active sites fully, which are also beneficial to transport and diffusion of products. In addition, highly uniform sizes and pore shapes of MOFs are important to size-selective catalytic reaction, which can effectively control the size of the participating molecules. However, the catalytic centers of MOFs are usually limited by the active group on the organic linkers and the coordinatively unsaturated metal sites-Lewis acid centers. Due to these factors, MOFs are limited at a certain catalytic activity. Fortunately, the pore space on MOFs can accommodate multiple additional active species as guests to produce MOF-based nanocomposites for catalytic reactions, such as metal nanoparticles, metal oxide nanoparticles, hemin, Prussian blue,
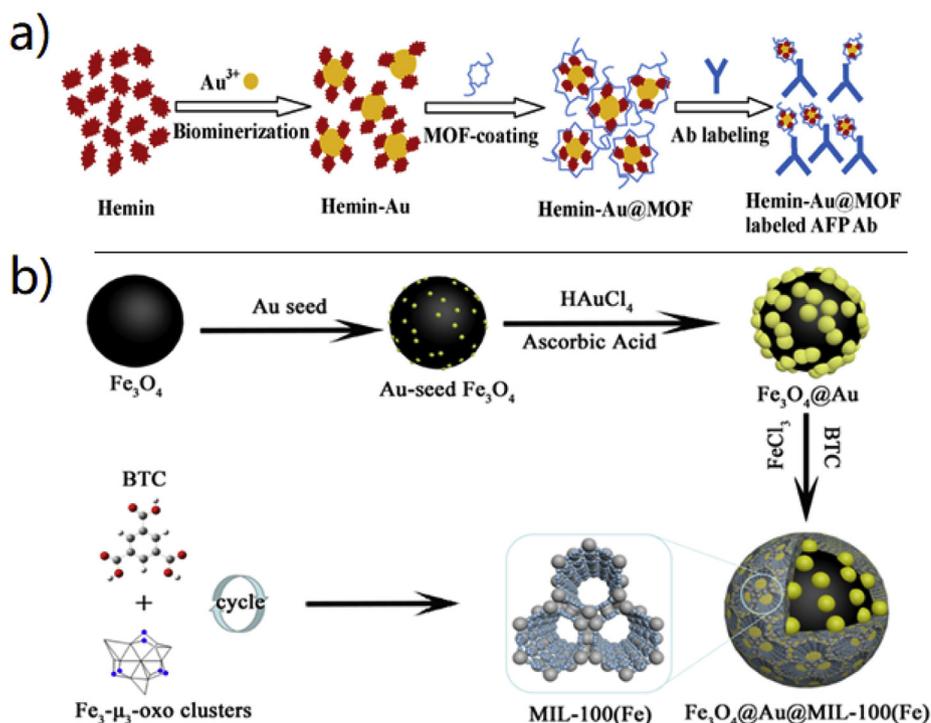


**Fig. 2.** (a) Scheminatic illustration of the fabrication procedure of Hemin-Au@MOF for labeling AFP antibody (Ab), including the hemin-mediated Au biomineriation yielding Hemin-Au, the coating of Tb-MOFs forming Hemin-Au@MOF, and the labeling of AFP Ab(Zhang et al., 2018d). (b) Schematic illustration of the magnetic MOF-based nanocatalyst synthetic process (Ma et al., 2018).

and enzymes(Jiao et al., 2018; Liang et al., 2019; Yang et al., 2017b)).

*2.1.3.1. 3D MOF-metal nanoparticles composites.* Metal nanoparticles (MNPs), particularly small MNPs, as effective catalysts have attracted wide attention due to their remarkable mimetic enzyme activities (e.g. catalase, oxidase, superoxide dismutase, and peroxidase)(Li et al., 2015). However, the high surface energy of MNPs can lead to the thermodynamic instability and easy aggregation of them in solution during catalytic reactions, and their catalytic activities decreased greatly (Yang et al., 2017b). However, the porous structure of MOFs can provide inherent conditions for stabilizing small MNPs, keeping them from the common aggregation and making catalysts possess a higher activity and a stronger stability. In addition, the development of MOF-MNPs composites also broadens the scope of catalytic reactions (Yang et al., 2017b). The doped noble MNPs in MOFs have been verified to significantly enhance the enzyme-like catalytic activity of MOFs, such as AuNPs, AgNPs, PdNPs, and PtNPs(Li et al., 2018c). For example, Shen and co-workers recently developed a novel AuNPs/Ce-MOFs, which was synthesized via decorating AuNPs in Ce-MOF. The AuNPs in Ce-MOFs nanocomposites not only could act as a nanocarrier to capture –SH terminated hairpin probes 2 (HP2) for obtaining HP2/AuNPs/Ce-MOFs signal probes, but also could act as the co-catalysts to catalyze the oxidation of ascorbic acid (AA)(Shen et al., 2016). A new Pt nanoparticles-functionalized Co-MOFs (PtNPs@Co(II)MOFs@PtNPs) was reported by Yang's group, which was prepared in two steps. First of all, the Co(II)MOFs@PtNPs were simply synthesized by using the mixed solvothermal strategy, encapsulating Pt nanoparticles (PtNPs) into the amino functionalized Co(II) MOFs materials. Then, assembling additional PtNPs on the external surface of Co(II)MOFs@PtNPs to produce PtNPs@Co(II)MOFs@PtNPs. The as-synthesized PtNPs@Co(II)MOFs@PtNPs could catalyze the oxidation of $H_2O_2$ with the improvement electron transfer of redox probe and could lead to the electrochemical signal amplification(Yang et al., 2017d). Zhang et al. reported a novel nanozyme decorated MOFs, namely PCN-224-Pt, which was simply prepared by homogeneously decorating Pt nanozymes on porphyrinic Zr-MOF nanoparticles. The PCN-224 (porous coordination network-224) was prepared through in situ reduction strategy, which could prevent the neighboring PtNPs aggregating and kept them stable, endowing the Pt nanozymes high stability and excellent catalase-like property. The as-synthesized PCN-224-Pt exhibited an excellent catalase-like activity and could catalyze the decomposition of $H_2O_2$ to generate $O_2$ with the existence of $H_2O_2$, going a step further to produce $^1O_2$ in the presence of light(Zhang et al., 2018j). Zhang's group recently successfully developed novel biomineralized Hemin-Au@MOF composites (Fig. 2a), which were synthesized through two steps. First, hemin was remolded with biomineralized gold to produce Hemin-Au core. Following that, Hemin-Au core was encapsulated into the Tb MOF matrix. The as-prepared Hemin-Au@MOF exhibited high environmental stability and double catalysis activities of gold catalysis and enhanced peroxidase-like (Zhang et al., 2018d).

It was reported that AuNPs and AgNPs exhibited remarkable surface-enhanced Raman scattering (SERS) activities. Encouraged by distinctive structure of MOFs, immobilizing the Au/AgNPs on the surface of MOFs as an efficient SERS substrate gradually was widely studied. For example, Jiang's group successfully prepared a novel SERS substrate AgNPs/MIL-101(Fe) via in situ fabrication of AgNPs on the external surface of MIL-101(Fe). The as-synthesized AgNPs/MIL-101(Fe) combined the numerous Raman hot spots between the great adsorption performance of MOFs and the high-density AgNPs and was used to the detect dopamine (DA) sensitively via using ABTS as a SERS marker based on their excellent peroxidase-like activity(Jiang et al., 2015). Recently, Ma and co-workers fabricated novel magnetic MOF-based nanocatalysts (Fe$_3$O$_4$@Au@MIL-100(Fe)) (Fig. 2b) through three-step strategy, including the solvothermal reaction, Au seed-induced growth process, and low-temperature cycling self-assembly. The as-obtained

magnetic Fe$_3$O$_4$@Au@MIL-100(Fe) was verified to possess an excellent peroxidase-like catalytic activity and could catalyze the oxidation of TMB/OPD to generate a color reaction with the presence of $H_2O_2$. In addition, the resultant Fe$_3$O$_4$@Au@MIL-100(Fe) also was used as a SERS substrate for monitoring the enhancement of the photoinduced catalytic property stemmed from ascorbic acid (AA)-assistance in the oxidation reaction of peroxidase mimics(Ma et al., 2018).

*2.1.3.2. 3D MOF-metal oxide nanoparticles composites.* Some 3D MOF-metal oxide nanoparticles composites were also reported to possess enzyme-like catalytic activity, Gao's group for the first time reported the magnetic Fe$_3$O$_4$ nanoparticles (NPs) possessed an intrinsic enzyme mimetic activity as natural peroxidases(Gao et al., 2007). By modifying metal oxide NPs on the outer surface of MOFs, it possibly makes metal oxide NPs obtain an enhanced catalytic activity, because the MOFs are capable of preventing metal oxide NPs aggregation and keep them stable. To obtain a novel Fe-based MOFs with high peroxidase-like activity, Li et al. successfully developed a new magnetic porous material (Fe$_3$O$_4$/MIL-101(Fe)) through an effective ultrasound-assisted electrostatic self-assembly method for decorating the cysteine (Cys) functionalized Fe$_3$O$_4$ MNPs on the external surface of MIL-101(Fe). The as-prepared Fe$_3$O$_4$/MIL-101(Fe) exhibited an excellent peroxidase-like property, which was used for the dimerization reaction of o-phenylenediamine (OPD) with the existence of $H_2O_2$ as an active heterogeneous catalyst(Jiang et al., 2016). Then, their group used the as-obtained Fe$_3$O$_4$/MIL-101(Fe) directly catalyzed luminol CL without additional oxidants and exhibited stronger catalytic ability that could be applied for quantitative detection of $H_2O_2$ in medical disinfectant and glucose in human serum samples(Qian Tang et al., 2018). Shortly afterwards, Hu's group successfully synthesized a core-shell artificial peroxidase through a solvothermal strategy, namely, Fe$_3$O$_4$@MIL-100(Fe), which exhibited an excellent peroxidase-like activity and could catalyze the oxidation of TMB to generated a blue product in the presence of $H_2O_2$(Wu et al., 2017b). In addition to Fe$_3$O$_4$ nanoparticles (NPs)-MOF composites, there are some other metal oxide nanoparticles-MOF composites reported, such as vanadium oxide-MOF (Cui et al., 2018). Farha and co-workers managed to immobilize vanadium oxide on Zr-MOFs to fabricate a new supported vanadium oxide catalyst by solvothermal deposition in MOFs (SIM), named V-NU-1000. The obtained V-NU-1000 showed an excellent catalytic activity reflected by using the oxidation of 4-methoxybenzyl alcohol under an $O_2$ atmosphere and was verified to have higher selectivity and conversion than that vanadium oxide supported on high surface area zirconia (V–ZrO$_2$). Moreover, the stability of V-NU-1000 was verified via recyclability and leaching tests, in which V-NU-1000 still retained equivalent catalytic ability as the fresh catalyst with no loss of metal loading in the recollected V-NU-1000.

*2.1.3.3. 3D MOF-hemin composites.* According to previous reports, hemin acts as the active center of numerous heme-proteins and exhibits the peroxidase-like property, which is usually used for catalysis as an excellent mimetic peroxidase. However, the limited catalytic lifetime hindered the development of hemin being used as catalyst owing to their dimerization and oxidative self-destruction in aqueous media. In order to solve this problem, a promising strategy was put forward, which was used to prepare novel heme-composites by decorating the hemin on suitable carrier materials to obtain a highly stable and catalytic biomimetic catalyst (Li et al., 2016a). For example, by encapsulating hemin into the MOFs (HKUST-1), Luo and co-workers successfully fabricated a new MOF-based solid catalyst, which showed a remarkable peroxidase-like catalytic activity inheriting from hemin and could catalyze the chemiluminescence(CL) reaction between $H_2O_2$ and luminol in the neutral condition. In addition, the hemin@HKUST-1 still preserved a high catalytic activity after eight catalysis cycles (Luo et al., 2015). Li and co-workers managed to design and successfully synthesized a novel hemin/ZIF-8 composite with peroxidase-like

activity through facile one-pot strategy, which utilized the chemical bond interactions between ZIF-8 and hemin molecules under a moderate condition in methanol medium. It was verified that hemin molecules were uniformly distributed in the framework of ZIF-8 because its mesoporous structure and the –COOH groups were connected with metal ions. In addition, through the microenvironment provided by ZIF-8, the as-prepared hemin/ZIF-8 exhibited an excellent peroxidase-like activity with a great dispersity in aqueous solution and could catalyze the oxidation of the peroxidase substrate TMB with the presence of $H_2O_2$(Li et al., 2016a). In a very recent study, Wang and co-workers reported the preparation of the Hemin-Au@MOF for the first time, which was successfully synthesized via remolding catalytic hemin molecules with biomineralized Au to produce Hemin-Au core, and was further encapsulated inside the Tb MOF matrix. The prepared Hemin-Au@MOF composites exhibited high stability and excellent double catalysis properties of gold catalysis and enhanced peroxidase-like. Moreover, the as-prepared Hemin-Au@MOF composites could show much higher intrinsic catalysis and stronger substrate affinity (lower Michaelis constants) than pristine hemin molecules and natural peroxidase, which was applied for two signal amplification methods of gold-catalyzed silver staining and hemin-catalyzed chromogenic reaction to detect the alpha-fetoprotein (AFP) in blood(Zhang et al., 2018d).

*2.1.3.4. Other 3D MOFs-based composites.* Prussian blue (PB) is a vital class of mixed-valence compounds made by iron ions coordinated with CN bridges, which possesses a remarkable peroxidase-like catalytic property towards $H_2O_2$. Nevertheless, there are two main constraints to the applications of PB, the one is the blue color of PB itself affecting the target signals, another constraint is due to the poor stability and easy aggregation in aqueous solution, which might lead to the decline of catalytic activity (Michopoulos et al., 2014). In order to solve the above problems, Cui and co-workers managed to synthesis a new nanosized porous PB/MIL-101(Fe) material by decorating PB at the exposed metal sites of the MIL-101(Fe) during the process of preparation, in which forming multiple coordination bonds between CN residues on the PB backbone and vacant $Fe^{3+}$ sites on the MIL-101(Fe) surface. The as-obtained PB/MIL-101(Fe) exhibited a remarkable peroxidase-like catalytic activity to catalyze the decomposition of $H_2O_2$ due to its large reaction surface area, abundant active sites and easy electron transfer (Cui et al., 2015b). Yin and co-workers successfully fabricated a novel hemeprotein-metal organic framework hybrid composite (H-MOFs) with peroxidase-like catalytic activity through using one-pot synthesis strategy to embed protein into MOF, which took bovine hemoglobin (BHb) and ZIF-8 as a model reaction system. The as-fabricated H-MOFs not only exhibited high stability and excellent catalytic activity, but also showed 423% enhancement in peroxidase-like catalytic property compared with free BHb(Yin et al., 2016). Recently, Hu's group managed to prepare new ZIF-8/Zn–Al layered double oxides (LDO) composites via using in-situ growth approach without adding supernumerary zinc source. The as-obtained composite showed high adsorption ability and remarkable photocatalytic degradation activity for methylene blue (MB) because the hierarchical porous structure was formed via the growth of ZIF-8 on surface of LDO (Hu et al., 2018a). In addition, the integrated nanozymes (INAzymes) have been developed widely via encapsulating natural enzymes together within confined frameworks, which could enhance the stability and catalytic activity of natural enzymes (Lei et al., 2018; Lian et al., 2017; Mehta et al., 2016). For example, Liu and co-workers reasonably designed a porous MOF (HP–PCN-224(Fe)) (Fig. 3) with intrinsic peroxidase-like property and tunable hierarchical porosity, which was successfully fabricated by a modulator-induced approach. The resulting product was not only used as the enzyme-immobilization matrix but also used as an effective peroxidase-like mimic, which could catalyze the cascade reactions with the immobilized natural enzyme. To improve pH and thermal stabilities of natural enzymes, glucose oxidase (GOx) was immobilized on HP-PCN-224(Fe) to prepare an excellent GOx@HP-PCN-224 (Fe) composite, which could catalyze the cascade reaction of ABTS and glucose. Similarly, immobilizing uricase on HP-PCN-224(Fe) could obtain a new uricase@HP-PCN-224 (Fe) composite.
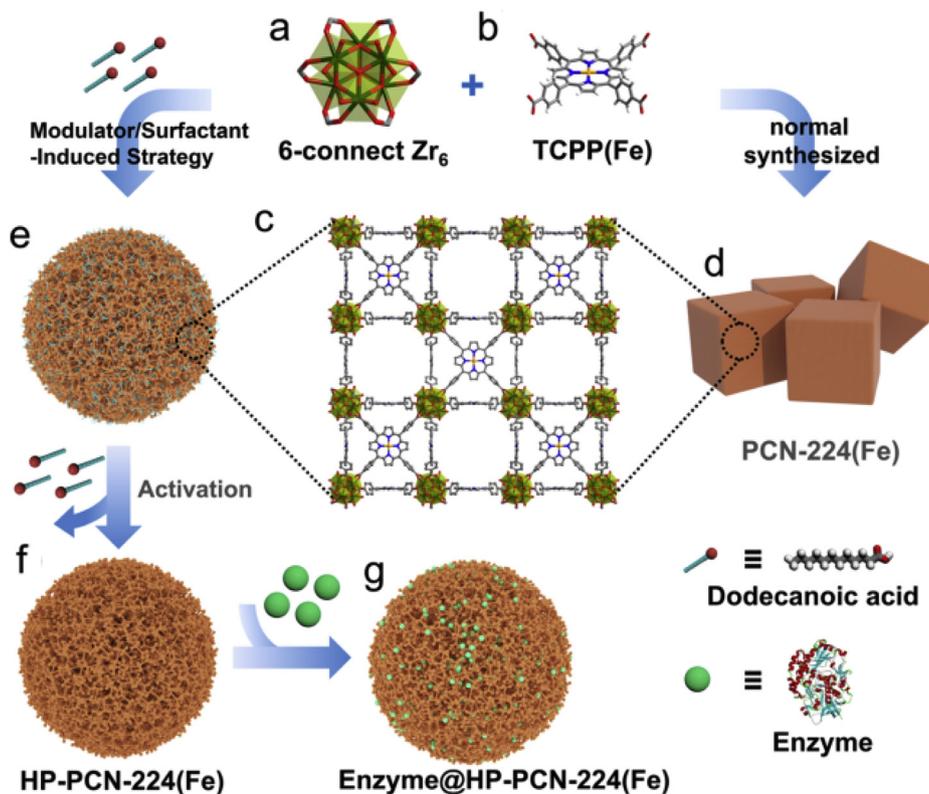


**Fig. 3.** Schematic diagram of the preparation of the mimic multienzyme system enzyme@HP-PCN-224(Fe)(Liu et al., 2018d).

The as-obtained uricase@HP-PCN-224(Fe) composite could be used for the cascade reaction of 4-aminophenazone/2,4-dichlorophenol sulfonate(DCPS) and uric acid (UA)(Liu et al., 2018d).

### 2.1.4. 3D MOF derivatives

As a class of crystalline nanoporous material with tailorable and diversified structures, MOFs have been used as versatile precursors/sacrificial templates to synthesize multiple MOF derivatives, including carbon-based materials, metal oxide/carbon composites, metal/carbon composites, etc. Compared to traditional nanoporous materials, MOF derivatives open up a novel avenue to the fabrication of diversified porous materials. MOF derivatives possess large surface area, enhanced stability, ordered porous structure, and easy adjustment of pore size, which endow them remarkable catalytic properties, even under harsh reaction conditions(Chen et al., 2018g; Liang et al., 2018c; Qian et al., 2017). MOF derivatives have been widely studied. For example, Wang's group developed a novel nanocomposite (CuNPs@C) with high peroxidase-like activity, which was successfully synthesized via using [Cu$_3$(BTC)$_2$](Cu-MOF) as a precursor, through a one-pot thermolysis strategy. The as-fabricated CuNPs@C not only possessed the merits of easy preparation and high stability, but also showed a strong affinity to H$_2$O$_2$. In addition, the as-synthesized nanocomposites exhibited an enhanced peroxidase-like activity to H$_2$O$_2$ compared to HRP, because Cu NPs were embedded into carbon matrix without aggregating (Tan et al., 2014). A series of HKUST-1 derivatives were systematically prepared by Yoon's group via using different reaction temperature and time. It was verified that high temperature and short time of carbonization reaction could result in the generation of partially oxidized Cu$_2$O species rather than pure Cu NPs. The Cu@C-500 was prepared at suitable carbonization temperature(500 °C), which possessed high surface area and hierarchical porosity. In addition, compared with Cu@C-400 and Cu@C-700, Cu@C-500 showed the highest peroxidase-like catalytic activity for glucose biosensing(Song et al., 2017). Huang and co-workers successfully synthesized a novel nanozyme (CoNPs/MC) via encapsulating Co NPs into MOFs (NH$_2$-MIL-88(Fe))-derived magnetic carbon (MC) material through in situ reduction approach. The prepared CoNPs/MC showed much higher peroxidase-like activity than pure magnetic carbon and Co NPs, and could catalyze the oxidation of TMB to produce a color reaction in the presence of H$_2$O$_2$(Dong et al., 2018). Recently, Huang and co-workers reported MOF-derived Co, N co-doped porous carbon hybrid with remarkable oxidase mimicking property for

the first time, which was synthesized via direct pyrolysis of the ZIF-67 precursor through one-pot strategy. ZIF-67 was used as both sacrifice template and nitrogen-rich carbon source. The Co$^{2+}$ ions coordinated to the organic ligand were reduced to form uniform Co NPs under the conditions of heat treatment. The obtained ZIF-67-derived Co, N-HPC showed an excellent oxidase-like activity owing to the well-dispersed Co NPs, abundant doped nitrogen, and highly N-doped hierarchically porous carbon. Moreover, the as-prepared product could efficiently catalyze the oxidation of TMB and 1, 2-diaminobenzene to generate a color change without the existence of H$_2$O$_2$ (Li et al., 2018d).

### 2.2. 2D MOFs-based nanozymes

#### 2.2.1. Pristine 2D MOFs

Compared to 3D MOFs, 2D MOFs with nanometer thickness are good for the diffusion of substrates and products. Moreover, benefit from lots of highly accessible active sites, 2D MOFs exhibit excellent catalytic activities. At present, a variety of 2D MOFs with catalytic property have also been reported (Cao et al., 2016; He et al., 2018b; Liu et al., 2018e; Wei et al., 2018; Ye et al., 2018; Zhao et al., 2018b; Zhao et al., 2015; Zhu et al., 2017). For example, Zhang et al. first reported the preparation of the ultrathin 2D bimetallic MOF nanosheets with biomimetic enzyme activity. Based on the surfactant-assisted synthetic approach, a series of 2D M-TCPP (Fe) (Fig. 4a) nanosheets were successfully prepared via using three kinds of metal nodes (M = Co, Cu, and Zn) and using TCPP (Fe) as organic linker. The as-obtained bimetallic 2D M-TCPP (Fe) nanosheets possessed the thickness of sub-10 nm. The 2D MOF nanosheets had the merits of large surface area, accessible active sites, and a small diffusion barrier for substrate molecules. Among these obtained 2D M-TCPP (Fe) nanosheets, the Co-TCPP (Fe) showed the best catalytic performance toward the reduction of H$_2$O$_2$(Wang et al., 2016b). In another work, Wei and co-workers successfully fabricated a series of 2D MOFs nanosheets (Fig. 4b) with excellent peroxidase-like activity via using binuclear paddle-wheel metal clusters and metalated TCPP ligands as raw materials. The as-synthesized 2D MOF nanozymes exhibited enhanced peroxidase-like activities compared to their 3D bulk analogues. The 2D MOF nanozymes could also be prepared via using the TCPP metalated with different metal ions (Cu$^{2+}$, Zn$^{2+}$, and Co$^{2+}$) as ligands. Among these obtained products, the 2D MOF architecture fabricated with the TCPP (Fe) ligands showed the highest catalytic activity, which demonstrated that the heme-like
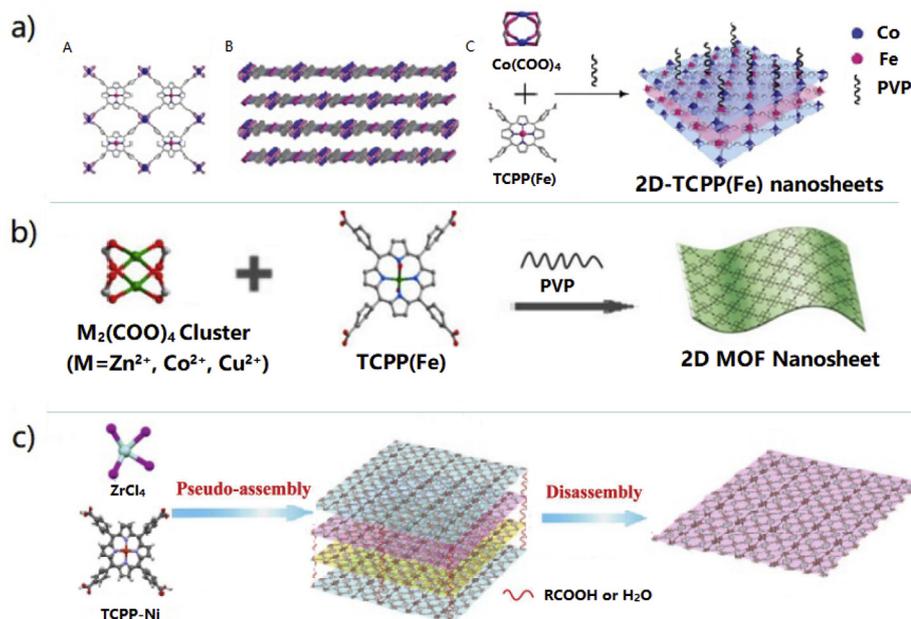


**Fig. 4.** (a) A, B Crystal structure of Co-TCPP(Fe) MOF. C, Schematic illustration of the surfactant-assisted synthesis of 2D Co-TCPP(Fe) nanosheets. TheMOF layers are drawn in blue and red, alternately, in order to make the layered structures more clear(Wang et al., 2016b). (b) Scheme showing the surfactant-assisted bottom-up synthesis of 2D MOF nanosheets(Cheng et al., 2017). (c) Schematic illustration for the synthesis process of UNs through pseudo-assembly–disassembly strategy(He et al., 2018b). (For interpretation of the references to color in this figure legend, the reader is referred to the Web version of this article.)

ligands played a dominant role on determining the activities of nano-zymes(Cheng et al., 2017). Recently, Hu et al. reported novel two-dimensional Ni-based MOF nanosheets with peroxidase-like activity, which were successfully fabricated via using simple solvothermal approach. The obtained ultrathin 2D Ni-MOF nanosheets exhibited an excellent peroxidase-like activity owing to their numerous active sites and ultrahigh specific surface area. In addition, the Ni-MOF nanosheets possessed high stability and good dispersity. According to catalytic mechanism analysis, it was demonstrated that the enzymatic kinetics of Ni-MOF nanosheets followed typical Michaelis-Menten theory. Moreover, the Ni-MOF nanosheets possessed high affinity to $H_2O_2$ and the peroxidase substrate (TMB), and could catalyze the oxidation of the substrate to generate a color reaction (Chen et al., 2018c). In order to enhance catalysis performance of MOF, He et al. synthesized zirconium-porphyrinic MOF nanosheets with ultrathin thickness by a pseudoassembly-disassembly approach (Fig. 4c). Compared to the corresponding bulk MOF, the as-obtained ultrathin nanosheets showed far superior photocatalysis property due to their unique properties stemming from highly exposed active sites and their ultrathin thickness (He et al., 2018b). In a very recent study, in order to explore the nanomaterial-based sensor arrays of phosphates, Wei and co-workers successfully synthesized a series of 2D-MOF nanozymes, the peroxidase-like activity of which could be modulated via various phosphates (AMP, ATP, PPi (pyrophosphate), Pi (phosphate), and ADP). Based on the effective modulation of the peroxidase-like activity of 2D-MOFs by phosphates, the sensor arrays were successfully constructed for the detection of phosphates both in biological samples and in aqueous solutions (Qin et al., 2018).

### 2.2.2. 2D MOFs with modification

2D MOF nanosheets possess numerous highly accessible active sites on their surface, which are beneficial for improving catalytic activity. In addition, 2D MOF nanosheets are modified easily by designing the organic ligands on MOFs, making MOFs possess different functions. For example, Hu and co-workers successfully synthesized a new amino-functionalized MOF ($NH_2$–Cu-MOF) by modifying amino on Cu-MOF through bottom-up synthesis method. The as-obtained $NH_2$–Cu-MOF nanosheets showed a high peroxidase mimic activity and could catalyze the oxidation of TMB with the presence of $H_2O_2$. Moreover, the as-prepared $NH_2$–Cu-MOF nanosheets also exhibited remarkable fluorescence property. Based on these properties, a biosensor for hypoxanthine detection was successfully developed (Hu et al., 2018b).

### 2.2.3. 2D MOF-based composites

*2.2.3.1. 2D MOF-metal nanoparticles composites.* Some metal nanoparticles (AuNPs, AgNPs, PtNPs, etc.) have been reported to possess intrinsic enzyme-like activity. Integrating MNPs with enzyme-like activity with 2D MOFs can endow the 2D MOFs with synergistic catalytic effects. For example, integrating two components with different catalytic activities could prepare multifunctional catalysts efficiently for cascade reactions. Huang and co-workers reported new 2D AuNPs/Cu-TCPP (M) hybrid nanosheets with peroxidase-like and GOx-like activities, which were fabricated via growing ultrasmall AuNPs on 2D metalloporphyrinic MOF nanosheets. In the as-obtained 2D AuNPs/Cu-TCPP(M) hybrid nanosheets, the 2D metalloporphyrinic MOF nanosheets was used as the peroxidase mimics and the ultrasmall AuNPs acted as GOx mimics. The 2D AuNPs/Cu-TCPP (M) hybrid nanosheets could not only catalyze the oxidation of glucose to generate gluconic acid and $H_2O_2$ with the presence of $O_2$, but also could catalyze the oxidation of TMB to produce a color change with the $H_2O_2$ generated in situ. Therefore, the resulting product could catalyze the cascade reaction without any natural enzymes and be used for detection of glucose (Huang et al., 2017b). Hu's group successfully developed a novel glucose electrochemical sensor, which was successfully fabricated by decorating AuNPs with the Ni-MOF/Ni/NiO nanocomposites. The obtained Ni-MOF/Ni/NiO nanocomposites were synthesized through

one-step calcination of Ni-MOF. Then, the numerous AuNPs were immobilized onto the surface of Ni-based nanocomposites through electrostatic adsorption. It was found that the AuNPs were well distributed on Ni-based nanocomposites' surface. The electrocatalytic property of Au–Ni nanocomposites was highly enhanced after functionalizing AuNPs onto them, which was verified by cyclic voltammetry study. Compared to Ni nanocomposite modified electrode, the as-obtained product showed enhanced electrocatalytic activity and high electron transfer rate towards the oxidation of glucose. In addition, the as-prepared product also exhibited other outstanding performances, including reproducibility, selectivity, and stability (Chen et al., 2018d). Lu and co-workers successfully fabricated a new 2D nanosheet of mixed-ligand MOF (NMOF-Ni), which was used as a good matrix to grow AuNPs for the first time. Attributed to the virtues of well-defined micropores and functional oxygen-decorated inner walls, the ultrasmall AuNPs with the size of around 1 nm were embedded within 2D NMOF-Ni nanosheets by solution impregnation. The obtained Au-1@NMOF-Ni composite showed remarkable catalytic activity and good size selectivity toward nitrophenol owing to the activity of Au NPs and the intact microporosity of 2D NMOF-Ni nanosheets (Yan et al., 2018). In a very recent work, Ying's group successfully fabricated Cu-TCPP (Fe) nanosheets through a surfactant-assisted synthetic strategy, in which $Cu_2(COO)_4$ paddle-wheel clusters, poly(vinylpyrrolidone) (PVP) and TCPP(Fe) were used as metal nodes, capped reagents and ligands, respectively. Then, growing ultrasmall and uniform PtNPs on the surface of ultrathin Cu-TCPP(Fe) nanosheets with thickness less than 10 nm to produce PtNPs/Cu-TCPP(Fe) hybrid nanosheets by a photochemical reduction way. Compared to PtNPs, Cu-TCPP (Fe) nanosheets, and the physical mixture of both, the prepared PtNPs/Cu-TCPP(Fe) hybrid nanosheets possessed an enhanced peroxidase-like catalytic activity due to the synergistic effect, and could catalyze the oxidation of TMB to form an impressive blue color (Chen et al., 2018a).

*2.2.3.2. 2D MOF-metal oxide nanoparticles composites.* Some metal oxide nanoparticles-2D MOF composites were also reported to possess enzyme-like catalytic activity. For example, Zhao and co-workers successfully prepared novel bimetallic $Fe_3O_4$ and AuNPs anchored 2D Cu-MOF nanosheets with bimetallic anchorage via using a simple two-step process at room temperature and ambient pressure, namely Cu (HBTC)-1/$Fe_3O_4$-AuNPs nanosheets. The synergistic coupling effect between MNPs and 2D Cu-MOF nanosheets lead an enhanced catalytic activity and affinity to substrates compared to MNPs anchored Cu-MOF nanosheets (without Fe alloying) or pristine 2D Cu-MOF nanosheets. The as-obtained Cu(HBTC)-1/$Fe_3O_4$-AuNPs nanosheets possessed an excellent peroxidase-like catalytic activity and good affinity for single-stranded DNA. Interestingly, the catalytic activity of resulting product could be flexibly regulated via the conformational variation of ssDNA (single-stranded DNA) owing to the change in the electrostatic interaction between catalysts and substrates upon the adsorption of negatively charged DNA on 2D Cu-MOF nanosheets by π-π stacking(Tan et al., 2017a)

*2.2.3.3. Other 2D MOFs-based composites.* In order to improve the stability and activity of natural enzymes, Lei et al. immobilized glucose oxidase (GOD) on the surface of 2D Co–Fe MOF to develop an integrated tandem catalyst system. The 2D Co–Fe MOF was successfully prepared with Co as node and TCPP (Fe) as linker and could be used as a matrix for the GOD immobilization. The as-synthesized GOD@Co-FeMOF complex possessed a highly stable activity and showed an excellent peroxidase-like catalytic activity, which was used to catalyze the oxidation of glucose to generate glucose acid and $H_2O_2$. Moreover, the resultant GOD@Co-FeMOF could drive a reaction cascade for in situ generation of NO by the oxidation of L-Arginine in physiological pH. In the existence of glucose and L-Arginine, NO could be produced continuously (Ling et al., 2018).
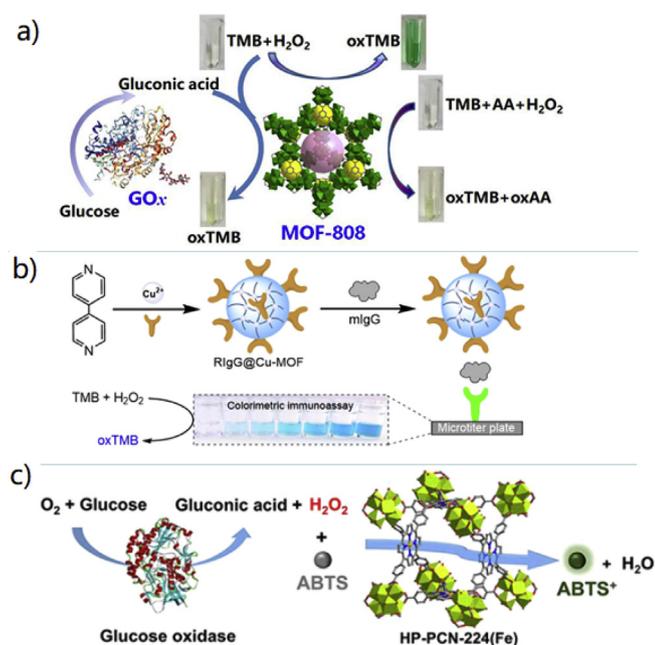
**Fig. 5.** (a) Principle of the colorimetric detection of AA, $H_2O_2$ and glucose based on the MOF-808(Zheng et al., 2018). (b) Illustration of the colorimetric immunoassay of mIgG based on RIgG@Cu-MOF as a detection antibody(Wang et al., 2018b). (c) Schematic diagram showing the tandem catalysis of GOx@ HP-PCN-224 (Fe)(Liu et al., 2018d).

Cui and co-workers successfully synthesized new $Ag_3PO_4$@UMOFNs core-shell photocatalysts via coating the UMOFNs (ultrathinning MOFs into two-dimensional nanosheets) on $Ag_3PO_4$ NPs. In UMOFNs, the metal clusters were connected by Ni–O–Co bonds, the metal centers and organic ligands were connected by Ni–O and Co–O bonds. The as-obtained $Ag_3PO_4$@UMOFNs exhibited an enhanced photocatalytic activity due to the synergistic effects. It was verified that the π-π bonds of the organic ligands and weak interactions between the core-shell structures accelerated charge transfer. Moreover, the separation of the photogenerated charges and the enhancement of catalytic activity could be promoted via matching energy-level structures and a sufficiently large contact area (Liang et al., 2018b).

### 2.2.4. 2D MOF derivatives

In order to develop a highly active and sustainable metal materials as oxygen evolution and hydrogen evolution reaction catalysts, Du et al. successfully synthesized a remarkably active transition-metal phosphide-carbon nanosheet composite(Co–P@NC-800), which was derived via carbonization and subsequent phosphorization of 2D cobalt porphyrinic MOF nanosheets. The as-prepared Co–P@NC-800 materials showed excellent electrocatalytic activities due to their unique structure, ultrafine CoP and $Co_2P$ NPs well dispersed in a nitrogen-doped graphitic carbon matrix (Zhai et al., 2017).

## 3. Applications of MOFs-based nanozymes

### 3.1. Sensing applications of MOFs-based nanozymes

MOFs-based nanozymes possess many remarkable properties, which have been extensively used for multiple analytical purposes. According to previous reports, the sensing applications of MOFs-based nanozymes mainly include colorimetric sensing, fluorescent sensing, chemiluminescent sensing, electrochemical sensing, and SERS sensing (Li et al., 2018c; Wang, 2017; Zhang et al., 2018k).

### 3.1.1. Colorimetric sensing

Colorimetric sensing has attracted wide attentions due to its easy read-out and fast visual determination via the naked eyes or low-cost portable instruments, which can be applied to detect some analytes based on the color change. One of important types of the colorimetric sensing mainly focuses on that enzyme/nanozyme catalyzes the chromogenic substrates such as TMB, ABTS, and OPD to generate color change (Kim et al., 2012; Xiong et al., 2015; Zheng et al., 2018). Attributed to its easy read-out and fast visual determination via the naked eyes or low-cost portable instruments, colorimetric sensing techniques have been widely studied for the detection of food safety, environmental monitoring, clinic diagnostics, biological technology, and public safety control and so on (Huang et al., 2019a; Phan et al., 2018; Ren et al., 2018; Tang and Li, 2017; Wu et al., 2018a; Yin et al., 2017; Zhang et al., 2018a). In recent years, MOFs-based nanozymes have been widely applied in colorimetric sensing (Liu et al., 2019a; Qin et al., 2018). It can be observed that multiple analytes can be detected by colorimetric sensing. For example, Liu et al. successfully fabricated a porous MOF (Fe-MIL-88NH₂) with intrinsic peroxidase-like activity for colorimetric sensing, which could quickly catalyze the oxidation of the peroxidase substrate TMB with $H_2O_2$ to generate a blue colored change for the detection of glucose in serum samples. Glucose could be linearly detected in the range from 2 μM to 300 μM with a low detection limit (LOD) of 0.48 μM, and the color variation of glucose response was also obviously observed via the naked eyes at concentrations as low as 2 μM (Liu et al., 2013). In contrast, by inhibiting the peroxidase-like catalytic activity of Fe-MIL-88A, Li and co-workers successfully developed a novel and universal colorimetric biosensing platform for detection of thrombin, which could efficiently catalyze the oxidation of TMB from colorless into a bright blue colored product. However, in the presence of thrombin and thrombin aptamer, the peroxidase-like catalytic activity of Fe-MIL-88A was strongly inhibited, realizing the colorimetric detection. On the basis of the obvious colorimetric variation, the linear range for thrombin was 10–80 nM and possessed a low detection limit as low as 0.8 nM via using the proposed strategy. Even observed by naked eyes, the limit of detection was as low as 10 nM(Wang et al., 2016c). Similarly, Zheng and co-workers successfully synthesized a stable MOF (MOF-808) with high intrinsic peroxidase-like activity, which could be used for the colorimetric sensing of AA, $H_2O_2$ and glucose (Fig. 5a). The LOD of $H_2O_2$ was 4.5 μM and the linear range was from 10 μM to 15 mM. Given the peroxidase-like activity of MOF-808 could be inhibited by AA, a novel colorimetric sensing platform for determination of AA was successfully developed. The LOD of AA was 15 μM, and the linear range was from 30 to 1030 μM. In the light of the strong inhibition effect produced via gluconic acid, a new and selective colorimetric sensing for detection of glucose was successfully established. The LOD of glucose was 5.7 μM, and the linear range was 5.7–1700 μM(Zheng et al., 2018). In addition, by integrating antibody with catalytic Cu-MOF, a dual-functional MOF/antibody composite (RIgG@Cu-MOF) was also successfully constructed, the prepared RIgG@Cu-MOF possessed excellent peroxidase-like activity and could serve as a signal amplification unit to perform a sensitive colorimetric immunoassay. The LOD of RIgG@Cu-MOF for mIgG was 0.34 ng/mL (Fig. 5b). Interestingly, integrating the natural enzymes with MOF was also a promising approach to design the mimic multienzyme systems for efficient colorimetric detection of the biomolecules (Fig. 5c)(Liu et al., 2018d). In order to develop novel sensor arrays for discriminating multiple phosphates simultaneously, Qin et al. fabricated a series of 2D-MOF nanozyme-based sensor arrays via utilizing their peroxidase-mimicking activity for the determination of various phosphates (Including AMP, ADP, ATP, PPi and Pi)(Qin et al., 2018) (Fig. 6a). In a very recent study, Ying and co-workers successfully prepared the new PtNPs/Cu-TCPP (Fe) hybrid nanosheets with peroxidase-like activity, which could efficiently catalyze the oxidation of TMB to produce a blue color product and could be applied for colorimetric sensing of $H_2O_2$ and glucose
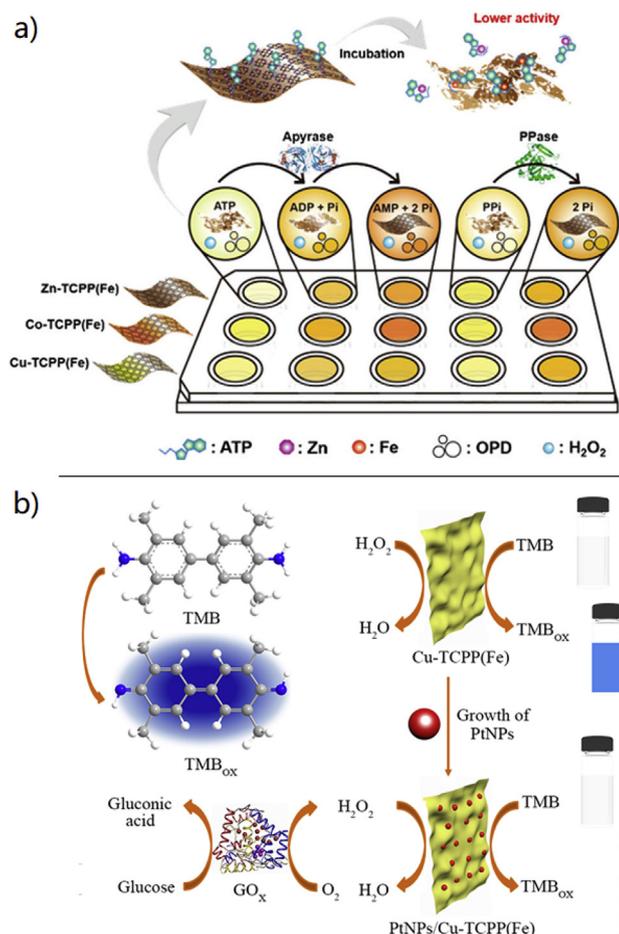
**Fig. 6.** (a) Schematic of 2D-MOF-Nanozyme sensor arrays probing phosphates and their related hydrolytic processes (Qin et al., 2018). (b) Schematic illustration of the synthesis method of PtNPs/Cu-TCPP (Fe) hybrid nanosheets and their application in colorimetric detection of $H_2O_2$ and glucose (Chen et al., 2018a).

(Fig. 6b). The LOD of $H_2O_2$ was 0.357 μM, and the linear range was 2–100 μM. There was a linear relationship with glucose concentration from 2 to 200 μM with a LOD of 0.994 μM(Chen et al., 2018a). Recently, Huang and co-workers successfully synthesized CoNPs/MC via embedding CoNPs into $NH_2$-MIL-88(Fe) MOFs-derived magnetic carbon (MC) through in situ reduction of cobalt precursors by $NaBH_4$. The obtained CoNPs/MC exhibited remarkable peroxidase-like activity and catalyzed the color reaction of TMB. On this basis, a new detection method of glucose was developed via combining GOx with CoNPs/MC for biosensing. The concentration of glucose was detected with a good linear relationship ranging from 0.25 to 30 μM and a lower LOD of 156 nM(Dong et al., 2018).

### 3.1.2. Fluorescent sensing

Fluorescent sensing is performed mainly based on the target analyte mediated fluorescence quenching or fluorescence enhancement, which possesses high sensitivity and selectivity for trace target analysis (Li et al., 2019b; Sadeghi et al., 2018; Majdinasab et al., 2019). In recent years, fluorescence sensing based on the MOFs-based nanozymes also has attracted widespread concern, because high catalytic properties of MOFs-based nanozymes can be used for the generation and amplification of fluorescence signals (Li et al., 2018b; Yi et al., 2016a; Zhao et al., 2016). For example, Tan and co-workers successfully prepared a novel Cu-based MOF (HKUST-1) with peroxidase-like activity, which could effectively catalyze non-fluorescent thiamine (TH) to generate a strong
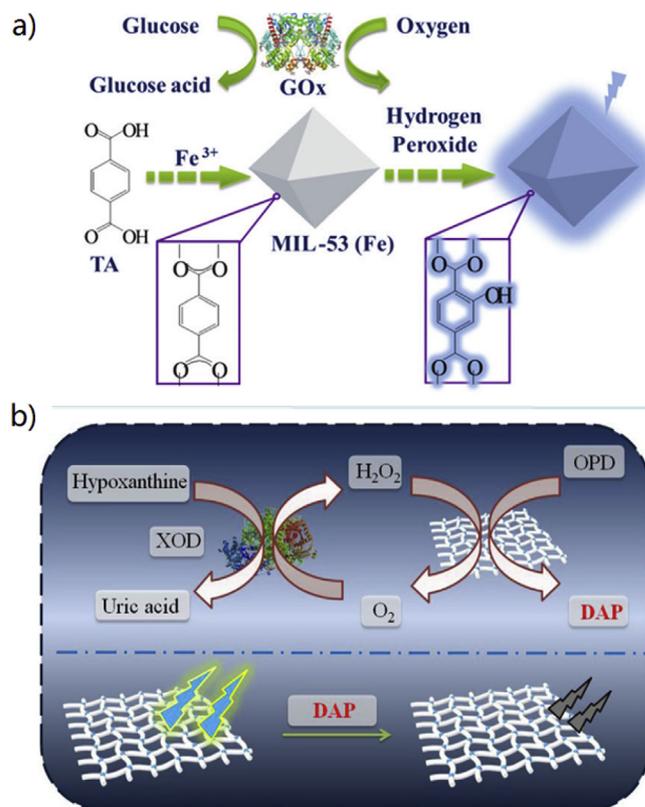


**Fig. 7.** (a) Principle of the fluorescence detection of glucose based on the bifunctional MIL-53(Fe) nanozyme (Lin et al., 2018b). (b) The principle of the biosensor based on $NH_2$–Cu-MOF nanosheet(Hu et al., 2018b).

fluorescence with the existence of $H_2O_2$. Based on the catalytic activity of HKUST-1, a sensitive and simple fluorescent approach for determination of TH was established. The concentration of TH could be detected was as low as 1 μM and the linear range was 4–700 μM. The LOD of TH was about 50 fold lower than the HRP-based fluorescent detection (Tan et al., 2015). Lin et al. successfully developed a new nanozyme MIL-53(Fe) with the peroxidase-like catalytic activity and fluorescence property, which was used for sensitive turn-on fluorescence detection of $H_2O_2$ and glucose (Fig. 7a). In their work, the as-obtained MIL-53(Fe) could activate $H_2O_2$ to generate ·OH and the produced ·OH could react with TA (the organic linker of MOF) to generate a fluorescent product, resulting in the enhancement of fluorescence. The detected concentration of $H_2O_2$ could be as low as 7.54 nM with a good linear relationship ranging from 0.5 to 24 μM(Lin et al., 2018b). Recently, Hu and co-workers successfully synthesized a novel aminofunctionalized two-dimensional MOF ($NH_2$–Cu-MOF) with peroxidase-like activity and fluorescence property (Fig. 7b). Based on two properties of $NH_2$–Cu-MOF, a new method for the detection of hypoxanthine was developed. The fluorescence intensity had a good linear relationship with the concentration of hypoxanthine ranging from 10 to 2000 μM, and the LOD was 3.93 μM(Hu et al., 2018b). In a very recent study, Hu et al. prepared a novel Cu-based two-dimensional MOF (CuBDC NS) with peroxidase-like activity. The obtained CuBDC NS could catalyze the oxidation of terephthalic acid to produce a blue-fluorescent product with the existence of $H_2O_2$. However, the pyrophosphate possessed a strong affinity for $Cu^{2+}$ and could block the peroxidase-mimicking activity of the CuBDC NS. Fortunately, the inorganic pyrophosphatase could hydrolyze the pyrophosphate and could gradually restore peroxidase-mimicking activity. On this basis, a strategy based on fluorescent sensing was successfully designed for the detection of the activity of inorganic pyrophosphatase. The fluorescence intensity had a good linear relationship with inorganic

pyrophosphatase activity ranging from 1 to 50 mU/mL, and the LOD was 0.6 mU/mL(Hu et al., 2019).

### 3.1.3. Chemiluminescent sensing

Chemiluminescent sensing as one of promising analytical techniques can be constructed based on the emission of light produced from a chemical reaction, which has been used for the detection of various targets due to its outstanding advantages of rapidity, easy operation, simple instrument without monochromator, wide linear range, and low LOD (Mao et al., 2018). Chemiluminescent sensing has provided a highly sensitive, simple, and flexible strategy for analysis (Chen et al., 2012; Gao et al., 2017b; Kong et al., 2017; Li et al., 2017b). MOFs-based nanozymes have also been studied as a promising catalyst for chemiluminescent sensing. For example, Chi's group successfully prepared new Hemin@HKUST-1 composites with excellent catalytic activity via encapsulating hemin into HKUST-1, which showed remarkable catalytic activity toward the luminol-$H_2O_2$ chemiluminescent system in neutral solution. Based on above chemiluminescent system, an excellent, green, selective and sensitive chemiluminescent sensor was developed for the determination of $H_2O_2$ and glucose. The linear detection range for $H_2O_2$ was from 5.0 to 1000 μM with a low LOD of 2 μM. The glucose could be detected as low as 7.5 μM, and had a good linear relationship ranging from 7.5 to 750 μM(Luo et al., 2015). Huang et al. reported that MIL-53(Fe) MOFs could remarkably enhance the chemiluminescence (CL) of luminol with the presence of $H_2O_2$ in an alkaline medium for the first time. The as-obtained MIL-53(Fe) MOFs showed excellent catalytic performance toward the luminol-$H_2O_2$ CL system and the CL intensity was about 20 times higher than that in luminol-$H_2O_2$ CL system. On this basis, a chemiluminescent method was established for the determination of glucose via coupling with GOx. A good linear relationship ranging from 0.1 to 10 μM was obtained with a limit of 0.05 μM for the detection of glucose(Yi et al., 2016b). Similarly, Li and co-workers found that Fe-MIL-88$NH_2$ MOFs could effectively enhance the chemiluminescence of luminol-$H_2O_2$ reaction due to their peroxidase-like activity. In addition, the Fe-MIL-88$NH_2$ MOFs could catalyze the decomposition of $H_2O_2$ to produce hydroxyl radical. The chemiluminescent intensity had a good linear relationship with the concentration of $H_2O_2$ ranging from 0.1 to 10.0 μM. The low LOD of $H_2O_2$ was 0.025 μM (Li et al., 2017c). Recently, Huang et al. successfully prepared new MOF-235/β-cyclodextrin (β-CD) hybrids, which showed high catalytic activity for the luminol-$H_2O_2$ CL system. A new chemiluminescent approach for the determination of glucose was constructed and the concentration of glucose was detected with a good linear relationship ranging from 0.01 to 3 μM and a low LOD of 0.01 μM(Mao et al., 2018).

### 3.1.4. Electrochemical sensing

The electrochemical sensing is established by the variation of output-electrical signals generated from the chemical reactions between electrode-immobilized recognition elements and target analytes, which can be used to achieve the qualitative detections and quantitative assays of target molecules through the production of electrical signals which is related to target analyte concentrations (Li et al., 2019b; Liu et al., 2019b; Ziyatdinova et al., 2018). To date, electrochemical sensing has been extensively studied and widely applied for multiple fields, such as food quality control, environmental monitoring, chemical treat detection and medical diagnostics(Kempahanumakkagari et al., 2018a; Liu et al., 2018b; Liu and Yin, 2016; Morozan and Jaouen, 2012). Recently, MOF-based nanozymes as a catalyst are studied for catalyzing the electrochemistry signal amplification (Chen et al., 2018d; Hou et al., 2018; Kempahanumakkagari et al., 2018b; Xie et al., 2018). For example, by assembling palladium nanoparticles on the surface of Fe-MIL-88$NH_2$ MOFs microcrystals, Li et al. successfully synthesized a new iron-based MOF (PdNPs@Fe-MOFs) with intrinsic peroxidase-like property, which was applied in electrochemical biosensor for ultrasensitive detection of microRNA-122 for the first time. Attributed to the
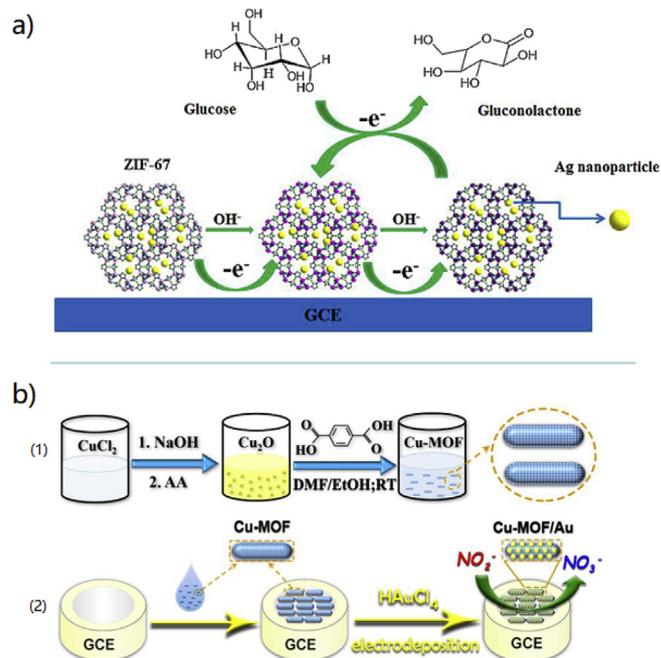


**Fig. 8.** (a) Schematic illustration of the electrooxidation of glucose to gluconolactone by Ag@ZIF-67 modified GCE in NaOH solution(Meng et al., 2018). (b) Schematic illustration for fabricating (1) Cu-MOF and (2) modified electrodes for nitrite sensing analysis(Chen et al., 2018b).

intrinsic peroxidase-like activity of PdNPs@Fe-MOFs, the signal of detection could be strongly enhanced towards the electrocatalytic oxidation of TMB with the existence of $H_2O_2$. With the assistance of target-catalyzed hairpin assembly and PdNPs@Fe-MOFs nanohybrids co-reaction for signal amplification, a wide detection range of microRNA-122 from 0.01 fM to 10 pM was achieved with a low LOD of 0.003 fM(Li et al., 2018e). Wang and co-workers fabricated a novel Ag@ZIF-67 nanocomposite, which was applied as the glucose electrochemical sensor for the first time (Fig. 8a). The obtained Ag@ZIF-67/GCE showed an enhanced electrocatalytic activity towards the oxidation of glucose and was used for the detection of glucose, and the concentration of glucose was detected with a good linear relationship ranging from 2 to 1000 μM with a low LOD of 0.66 μM(Meng et al., 2018). Berchmans and co-workers successfully a novel Cu based MOF with intrinsic peroxidase-like property, which was used to modify GCE (glassy carbon electrode) for the sensitive detection of $H_2O_2$ and glucose. On this basis, the concentration of $H_2O_2$ was detected with a good linear relationship ranging from 25 to 30000 μM with a low LOD of 25 μM(Menon et al., 2018). In a very recent study, Li et al. successfully fabricated a new nanocomposite (Cu-MOF/Au), which exhibited excellent synergetic catalytic effect for the oxidation of nitrite owing to the large surface area and porosity of Cu-MOF. The as-prepared Cu-MOF/Au with the merits of high sensitivity, selectivity and good stability could be used as an electrochemical sensing platform for quantitative detection of nitrite (Fig. 8b). It showed two wide linear ranges of 0.1–4000 and 4000–10000 μM with a low LOD of 82 nM for the detection of nitrite (Chen et al., 2018b).

### 3.1.5. SERS sensing

SERS sensing as an emerging and powerful analytical technology attracted wide attentions, which has been rapidly developed for biosensing, due to the remarkable advantages such as fingerprint information, in situ noninvasive detection, and ultrahigh sensitivity. Recently, SERS sensing has been successfully employed to achieve a sensitive assay of target molecules by using nanozymes to enhance the

SERS activities (Jiang et al., 2018; Zong et al., 2018). To enhance the SERS activities, integrating AuNPs and AgNPs into MOFs for the preparation of nanozymes is a promising strategy. For example, Li et al. successfully developed a novel efficient SERS substrate via in situ synthesis of silver nanoparticles (AgNPs) on the surface of MIL-101 (Fe). The as-fabricated AgNPs/MIL-101 (Fe) hybrid combined the numerous Raman hot spots between the high-density AgNPs and the good adsorption property of MOFs, making it an excellent SERS substrate for ultrasensitive SERS detection by effectively concentrating analytes in close proximity to the Raman hot spots domains between the adjacent AgNPs. The synthesized AgNPs/MIL-101 (Fe) hybrid with peroxidase-like activity was applied for ultrasensitive SERS detection of dopamine (DA) via using AZBTS as a SERS marker (Fig. 9a). The novel developed approach exhibited a good linear relationship ranging from 1.054 pM to 210.8 nM for DA with a low LOD of approximately 0.32 pM(Jiang et al., 2015). Hu et al. successfully synthesized new AuNPs@MIL-101 nanozymes via in situ growing AuNPs into a highly porous and thermally stable MIL-101. The prepared AuNPs@MIL-101 nanozymes showed an excellent peroxidase-like activity and could oxidize Raman-inactive reporter leucomalachite green into the active malachite green (MG) with the presence of $H_2O_2$, and simultaneously acted as the SERS substrates to enhance the Raman signals of the as-produced MG. By immobilizing glucose oxidase (GOx) and lactate oxidase (LOx) onto AuNPs@MIL-101, AuNPs@MIL-101@GOx and AuNPs@MIL-101@LOx integrative nanozymes were prepared for in vitro detection of glucose and lactate by SERS (Fig. 9b). In addition, the integrative nanozymes were used for monitoring the variation of glucose and lactate in living brains. The concentration of glucose was detected with a good linear relationship ranging from 100 to 200 μM and a low LOD of 4.2 μM. The concentration of lactate was detected with a good linear relationship ranging from 100 to 200 μM and a low LOD of 5 μM(Hu et al., 2017b). In a very recent study, Ma et al. successfully fabricated new SERS-active magnetic MOF-based nanocatalysts (Fe₃O₄@Au@MIL-100(Fe)) by a three-step way. The as-fabricated magnetic Fe₃O₄@Au@MIL-100 (Fe) nanocatalysts not only showed excellent peroxidase-like activity, but also could be used as a SERS substrate. Based on these characteristics, the fabricated magnetic nanocatalysts could be applied for monitoring in situ catalytic oxidation of TMB by $H_2O_2$ via using a SERS technique and the concentration of $H_2O_2$ can also be sensitively detected(Ma et al., 2018).

### 3.2. MOFs-based nanozymes for therapy

On the basis of previously published literatures, MOFs have been widely and intensively studied in cancer therapy applications, such as drug delivery, (photodynamic therapy) PDT, photothermal therapy (PTT), sonodynamic therapy (SDT), chemotherapy, oxidationtherapy, and radiotherapy (RT)(Cai et al., 2019; Chen et al., 2017b; Gao et al., 2018; Guan et al., 2018; Lan et al., 2017; Liu et al., 2018c; Lu et al., 2018b; Ni et al., 2018; Yang et al., 2017c; Zhang et al., 2018g; Zhou et al., 2018c). There have been already some literatures well summarizing the applications of MOFs in cancer therapy (Guan et al., 2018; Lan et al., 2019; Lu et al., 2018a; Wu and Yang, 2017). However, MOFs-based nanozymes catalytic mediated cancer therapies are rarely summed up. Based on the catalytic properties of MOFs-based nanozymes, some promising strategies have been developed for cancer therapy purposes. Herein, we mainly summarize MOFs-based nanozymes catalytic mediated cancer therapies, including cancer starvation therapy, enhancing photodynamic therapy, and synergistic therapy of both. In addition, the MOFs-based nanozymes for some other therapies are also simply summarized (Hartshorn et al., 2018; Lu et al., 2018a; Rojas et al., 2018; Wu et al., 2018b).

When cancer cells can't obtain sufficient nutrients and oxygen, they won't sustain their fast growth and proliferation, even starve to death, which is defined as cancer-starvation therapy. The cancer cells are starved to death via blocking the tumor nutrient supply or consuming intratumoral oxygen, which is a potentially useful strategy for treating cancer and has drawn great interest in recent years (Fu et al., 2018; Zhang et al., 2017a; Zhou et al., 2018a). Recently, MOFs-based nanozymes for cancerous starvation therapy have been researched hotly. For example, Zhang et al. successfully fabricated a novel biomimetic nanoreactor for cancer-starvation therapy via encapsulating GOx and prodrug tirapazamine (TPZ) in an erythrocyte membrane cloaked MOF nanoparticle (TGZ@eM), the as-prepared TGZ@eM nanoreactor could assist the delivery of GOx to tumor cells and exhausted glucose inside the tumor cells to block the tumor nutrient supply efficiently (Fig. 10a). Moreover, the prepared TGZ@eM nanoreactor could catalyze the oxidation of glucose and consume oxygen at the same time, this process could lead to the hypoxia inside the tumor cells, the resulting tumor hypoxia via starvation therapy further initiated the activation of prodrug tirapazamine (TPZ), which was released from the nanoreactor for enhanced colon cancer therapy(Zhang et al., 2018e). In addition to blocking the supply of oxygen and glucose to starve cancer cells, reducing the supply of ATP was also applied for cancer-starvation therapy. In a very recent study, Qu and co-workers rationally design and successfully fabricated new uniformly dispersed ultrasmall nanozymes (MOF-derived CeO₂ nanozymes) for the first time via using well-ordered crystalline metal organic frameworks (MOFs) as precursors. The as-obtained MOF-derived CeO₂ nanozymes possessed high oxidase-like property, ATP deprivation capability, and porous structure endowed them with strong oxidative damage function, higher drug loading capacity, and the ability of reducing energy supply(Fig. 10b). Attributed to the high deprivation abilities toward ATP and the excellent oxidase-like activity of MOF-derived CeO₂ nanozymes, the supply of ATP was efficiently reduced and blocked, a novel strategy was developed for safe and efficient synergistic cancer therapy both in vitro and in vivo(Cao et al., 2018).

In recent years, MOFs have been widely applied for cancerous photodynamic therapy (PDT) via integrating photosensitizers, which cause cytotoxic effects on cancer cells via converting the oxygen inside
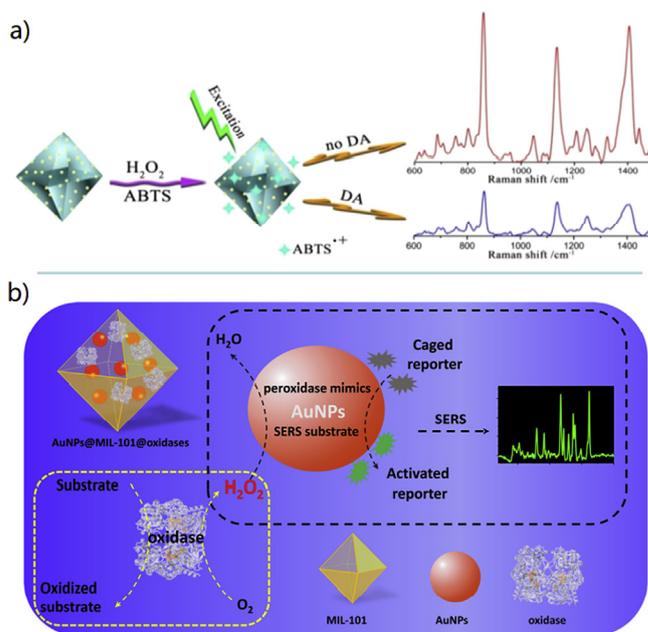


**Fig. 9.** (a) Schematic Diagram of Detection of DA Based on SERS(Jiang et al., 2015). (b) Schematic illustration of AuNPs@MIL-101@oxidases for efficient enzymatic cascade ereactions. First, oxidases catalyzed the oxidation of a substrate target (i.e., glucose or lactate) to produce $H_2O_2$; peroxidase-like AuNPs in AuNPs@MIL-101@oxidases then catalytically oxidized caged Raman reporters (i.e., LMG) with $H_2O_2$ to produce active Raman reporters (i.e., MG) and simultaneously enhanced the reporters' Raman signals for SERS measurements (Hu et al., 2017b).

**Fig. 10.** (a) Schematic illustration of the preparation of the (A) TGZ@eM nanoreactor and (B) erythrocyte membrane cloaked MOF biomimetic nanoreactor for starvation-activated colon cancer therapy(Zhang et al., 2018e). (b) Rational design and synthesis of n-CeO₂ NSs with enhanced oxid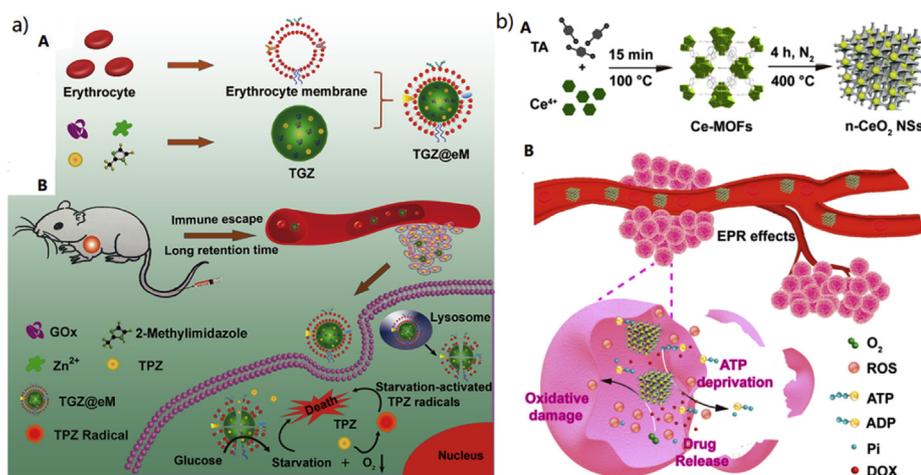ase-Like activity (A), as well as their usage as an efficient multifunctional platform for synergistic cancer therapy (B)(Cao et al., 2018).

the tumor cells into singlet oxygen ($^1O_2$). Nevertheless, the tumor hypoxia greatly limited the PDT efficiency of MOFs. Therefore, MOFs-based nanozymes have been studied for enhancing photodynamic therapy of cancer. The MOFs-based nanozymes with catalase-like activity could be used for the decomposition of intratumoral $H_2O_2$ and generating oxygen in situ inside the tumor, leading to a greatly enhanced PDT efficiency (Lan et al., 2018; Liu et al., 2018a; Zhang et al., 2018b). For example, Zhang et al. successfully prepared a novel composite of nanozymes (PCN-224-Pt) via decorating Pt nanozymes on photosensitizer integrated MOFs. The as-fabricated composites of nanozyme exhibited high stability and excellent catalase-like activity, which could induce the decomposition of intratumoral $H_2O_2$ to generate $O_2$ at the hypoxic tumor site, which was able to utilize the production of cytotoxic $^1O_2$ by PCN-224-Pt to damage cancer cells seriously. On this basis, a versatile nanoplatform for enhancing photodynamic therapy was successfully developed and promoted the applications of MOFs-based nanozymes in modern oncology (Fig. 11a) (Zhang et al., 2018j). Recently, Qu and co-workers constructed a new-style versatile zirconium-ferriporphyrin MOF (Zr–FeP MOF) nanoshuttles through a facile one-pot hydrothermal strategy. The as-prepared nanoshuttles could enable simultaneously to produce abundant reactive oxygen species including hydroxyl radical (·OH) and singlet oxygen ($^1O_2$) for fighting cancer(Zhang et al., 2018c) (Fig. 11b).

Cancer-cell growth and proliferation require sufficient nutrients and energy supply, blocking the supply of energy and nutrients to starve cancer cells is an effective strategy for fighting cancer (Huo et al., 2017; Lin et al., 2018a). However, it is very difficult to completely eliminate tumors with starvation therapy alone, because tumor cells can get the continuous supply of energy and nutrients from the capillaries. During the process of tumor starvation therapy, MOFs-based nanozymes with GOx/GOx-like catalytic activity will catalyze the oxidation of glucose to produce $H_2O_2$, but oxygen is consumed and increase tumor hypoxia. The oxygen-dependent PDT is hindered by tumor hypoxia. Luckily, MOFs-based nanozymes with catalase activity can promote the decomposition of the produced $H_2O_2$ to generate $O_2$, which not only accelerates the oxidation of glucose by GOx but also enhances the generation of cytotoxic $^1O_2$ under light irradiation. Therefore, the preparation of MOFs-based nanozymes with GOx/GOx-like and catalase activity has the great potential to construct a cascade bioreactor for cancer starvation and photodynamic synergistic therapy. For example, Li et al. successfully constructed a novel cancer targeted cascade bioreactor (mCGP) for synergistic cancer starvation and photodynamic therapy via integrating GOx and catalase into the cancer cell membrane-camouflaged porphyrin MOF (PCN-224) (Fig. 12). The cancer targeting and retention abilities of mCGP were remarkably enhanced due to biomimetic surface functionalization. When the mCGPs with GOx and catalase activity were internalized by cancer cells, they could

not only catalyze the endogenous $H_2O_2$ to produce $O_2$, but also could accelerate the decomposition of intracellular glucose and remarkably enhance the generation of cytotoxic $^1O_2$ under light irradiation. The as-prepared mCGP showed amplified therapeutic effects of long-term cancer starvation and photodynamic synergistic therapy, which could efficiently inhibit the growth of tumors (Li et al., 2017a).
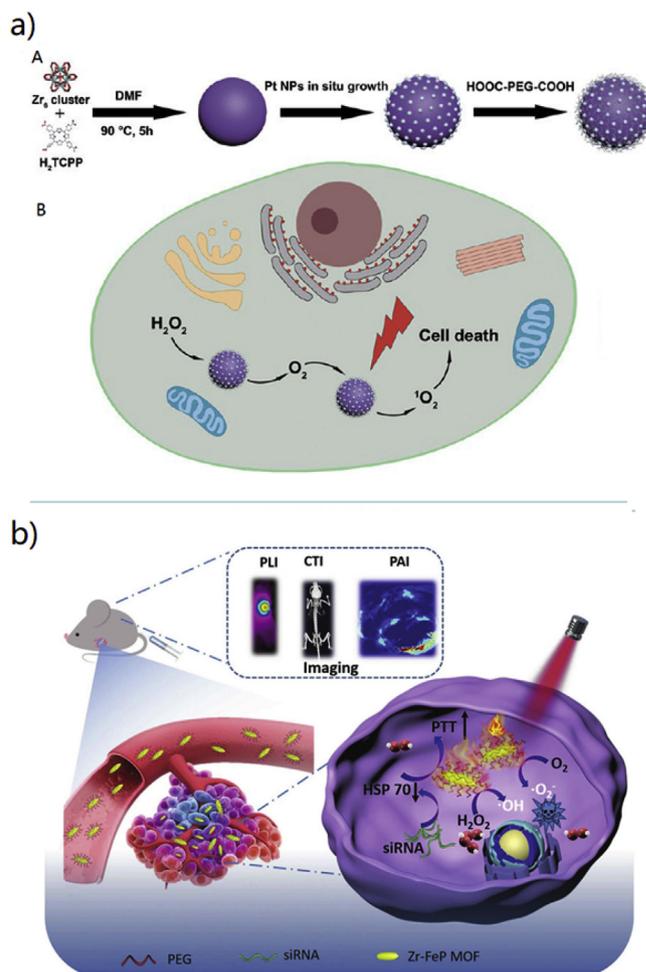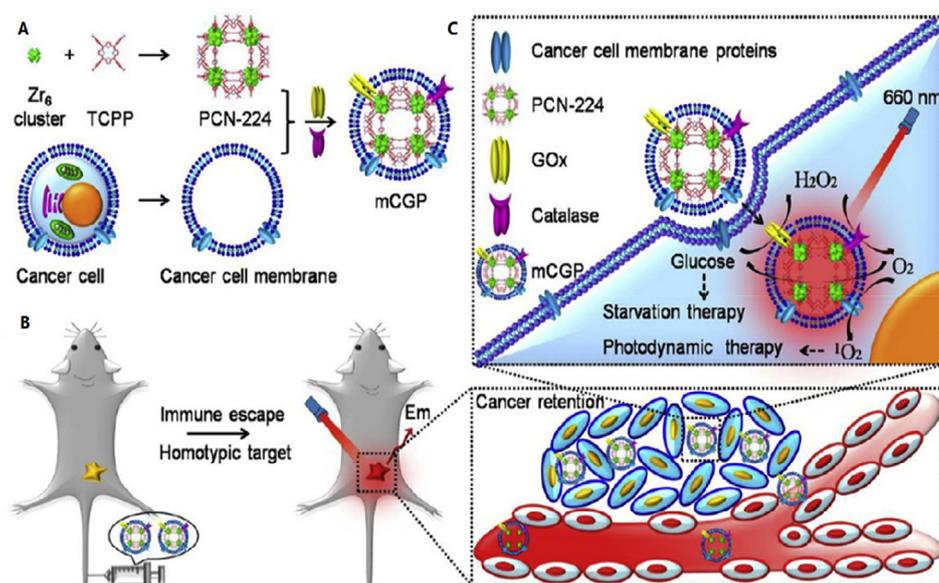


**Fig. 11.** (a) Schematic illustration of (A) the preparation process of PCN-224-Pt and (B) the use of PCN-224-Pt for enhanced PDT(Zhang et al., 2018j). (b) Schematic illustration of siRNA/Zr–FeP MOF nanoshuttles for multimode imaging diagnosis and combination of low-temperature PTT and PDT for cancer treatment(Zhang et al., 2018b).

**Fig. 12.** Schematic illustration of the cancer cell membrane camouflaged cascade bioreactor for cancer targeting starvation therapy and PDT. (A) The preparation processes of mCGP. (B) The immune escape and homotypic targeting abilities of mCGP endowing cancer accumulation and retention behaviors after intravenous injection. (C)The cascade reactions would amplify the synergistic effects of mCGP to cut off the cancer cell glucose supply for starvation therapy and promote $^1O_2$ generation for PDT under light irradiation (Li et al., 2017a).

According to previous reports, MOFs-based nanozymes have been also exploited for some other diagnosis and treatment of diseases (Fig. 13a)(Chen et al., 2015; Li et al., 2016b; Wang et al., 2016c). For example, Cheng et al. rationally designed and successfully developed a new GOx/Hemin@ZIF-8 nanozyme with remarkably enhanced catalytic activity and excellent stability as an integrative analytical platform for in vivo continuously monitoring the dynamic variations of stratum glucose in the brain of living rats following ischemia/reperfusion (Cheng et al., 2016). Cheng et al. successfully synthesized a series of MOF nanosheets with peroxidase-like catalytic activity as a highly sensitive and selective diagnostic platform for the monitoring of heparin (Hep) activity in live rats. The resultant 2DMOF nanosheets could physically adsorb Hep-specific AG73 peptides, the active sites of which were blocked. The catalytic activity of AG73-MOF nanosheets was restored upon the binding of Hep due to the highly specific interaction between AG73 and Hep. Based on the good biocompatibility and
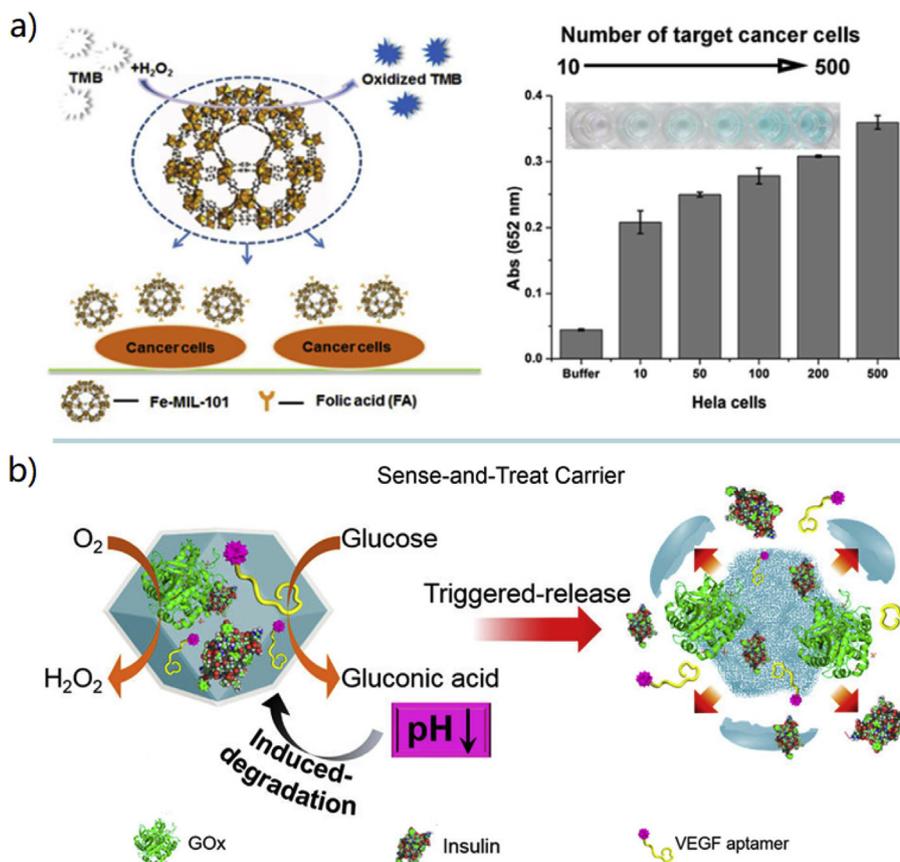


**Fig. 13.** (a) The detection of cancer cell based on the Fe-MIL-101(Chen et al., 2015). (b) Principle of the "sense-and treat carrier" based on the GOx/Hemin@ZIF-8 nanozymes(Chen et al., 2018e).

excellent diagnostic property endowed by AG73-2D MOF nanosheets, the process of eliminating Hep in vivo could be quantitatively monitored via coupling with microdialysis technology (Cheng et al., 2017). Chen et al. successfully prepared new glucose-responsive nanocomposites (GOx-loaded ZIF-8 NMOFs), which could be used as autonomous, sense-and-treat vehicles for controlling diabetes or macular diseases (Fig. 13b). The GOx and insulin could be loaded in the ZIF-8NMOFs. The resulting product could catalyze the oxidation of glucose to produce gluconic acid and $H_2O_2$, and formed an acidified microenvironment, which could lead to the degradation of the nanocomposites and the release of the loaded drugs for therapies (Chen et al., 2018e).

## 4. Conclusions and future outlooks

MOFs-based nanozymes as novel emerging and rapidly growing field have gained numerous achievable outcomes. In this review, we have summarized the recent achievements in the design strategies and multi-application of MOFs-based nanozymes, including the design strategies of 3D/2D MOFs-based nanozymes, sensing applications and therapeutic applications of MOFs-based nanozymes. Although a great deal of achievements have already been obtained in MOFs-based nanozymes, compared to the rapid development of MOFs in other fields, the researches of this field are still limited at an infant stage and are facing numerous challenges. In order to promote the development of design strategies and applications in MOFs-based nanozymes, the following challenges and obstacles should be considered in future studies:

(1) MOFs-based nanozymes have attracted the wide attentions, and have been successfully developed via various strategies. However, the catalytic activities of MOF-based nanozymes are far lower than that of the natural enzyme, which may attribute to the micro pores and the steric hindrance of MOF. Owing to these defects, larger molecule substrate can't enter the micro pores to participate in the catalytic reactions, leading to the decline of catalytic efficiency of MOF-based nanozymes (Lian et al., 2017; Yang et al., 2017b). To overcome these issues, synthesis of mesoporous MOFs with large cavities for the preparation of MOF-based nanozymes is a promising strategy. In addition, the development of 2D MOFs-based nanozyms with ultra-large specific surface area and larger active sites for substrates contact may solve this problem to a certain degree (Chen et al., 2018a; Huang et al., 2017b; Ling et al., 2018). There are many MOFs used as hosts to prepare the MOFs-based nanozymes and the great progress have been made. Integrating metal NPs, natural enzymes and nanozymes into MOFs for obtaining MOFs-based highly active nanozymes is a promising strategy and has become a hot spot in catalysis, but the mechanism of interactions between them still need to be explored. Moreover, among these MOFs used as hosts, the 2D MOFs are rarely reported. Compared to the traditional 3D MOFs, 2D MOFs possess larger surface areas and more accessible active sites. The nanozymes prepared by 2D MOFs can lead to higher speed and sensitivity of catalytic reactions. Therefore, focusing on developing 2D MOFs-based nanozymes is also a key to enhance catalytic activity of MOFs-based nanozyms (Chen et al., 2018a; Huang et al., 2017a; Li et al., 2018c).

(2) Most of MOFs-based nanozymes could hardly catalyze one specific substrate like natural enzymes with selectivity and specificity due to the lack of a substrate binding pocket. Molecular imprinting technology has been reported as a potential technology to improve the specificity of nanozymes (Chen et al., 2011; Zhang et al. 2017b, 2017c). Anchoring the molecularly imprinted polymers onto nanozymes is a promising method to prepare the nanozymes with high specificity (Fan et al. 2017, 2018; Zhang et al., 2017c), which would open a new avenue for MOFs-based nanozymes to increase the specificity and catalytic activity (Fan et al., 2017; Zhang et al., 2017c). Thus, MOFs-based nanozymes with selectivity and specificity remain to be studied. In addition, most of MOFs-based

nanozymes have been verified to possess oxidase-like catalytic activity, some even can be used for realizing a cascade reaction, but the catalytic mechanisms of them remain to be investigated. Moreover, most of the reported MOFs-based nanozymes only possess an oxidase-like catalytic activity currently, the diversity of which is very monotonous compared to natural enzymes. Therefore, realizing the diversity of MOFs-based nanozymes is also crucial. Some MOFs-based nanozymes with new catalytic properties are urgently developed, such as synthetase and hydrolase (Wu et al., 2018b).

(3) Although MOFs-based nanozymes have been successfully applied for cancer therapy and other therapies, there are some various problems to be solved, such as immunogenicity, biocompatibility clinical toxicity, and poor pharmacokinetics profiles. Before MOFs-based nanozymes are applied for clinical translation, these long-term effects of them should firstly be verified in animal models. In addition, MOFs-based nanozymes have been widely applied for cancer starvation therapy and have made great progress. However, it is very difficult to completely eliminate tumors with starvation therapy alone, because tumor cells can get the continuous supply of energy and nutrients from the capillaries. Therefore, it is a promising approach for improving treatment efficacy via combining starvation therapy with multiple synergistic therapies, such as PDT, PTT, SDT, immunotherapy, chemotherapy, gas therapy, and oxidationtherapy. Moreover, the mechanism of multiple synergistic therapies between each therapy modality should be expounded in detail to apply for clinical translation (Fu et al., 2018; Hartshorn et al., 2018; Rajendrakumar et al., 2018; Zhu et al., 2018).

## Conflict of interest

We declare that we do not have any commercial or associative interest that represents a conflict of interest in connection with the work submitted.

## CRediT authorship contribution statement

**Xianlong Zhang:** Conceptualization, Writing - original draft. **Guoliang Li:** Supervision, Writing - review & editing. **Di Wu:** Software. **Xiuling Li:** Software. **Na Hu:** Formal analysis. **Jian Chen:** Visualization. **Guang Chen:** Supervision. **Yongning Wu:** Supervision.

## Acknowledgement

## References

Ahmed, I.N., Yang, X.-L., Dubale, A.A., Li, R.-F., Ma, Y.-M., Wang, L.-M., Hou, G.-H., Guan, R.-F., Xie, M.-H., 2018. Hydrolysis of cellulose using cellulase physically immobilized on highly stable zirconium based metal-organic frameworks. Bioresour. Technol. 270, 377–382.

Ai, L., Li, L., Zhang, C., Fu, J., Jiang, J., 2013. MIL-53(Fe): a metal–organic framework with intrinsic peroxidase-like catalytic activity for colorimetric biosensing. Chem. Eur J. 19 (45), 15105–15108.

Bagheri, N., Khataee, A., Habibi, B., Hassanzadeh, J., 2018. Mimetic Ag nanoparticle/Zn-based MOF nanocomposite (AgNPs@ZnMOF) capped with molecularly imprinted polymer for the selective detection of patulin. Talanta 179, 710–718.

Cai, H., Huang, Y.-L., Li, D., 2019. Biological metal–organic frameworks: structures, host–guest chemistry and bio-applications. Coord. Chem. Rev. 378, 207–221.

Cao, F., Zhang, Y., Sun, Y., Wang, Z., Zhang, L., Huang, Y., Liu, C., Liu, Z., Ren, J., Qu, X., 2018. Ultrasmall nanozymes isolated within porous carbonaceous frameworks for

synergistic cancer therapy: enhanced oxidative damage and reduced energy supply. Chem. Mater. 30 (21), 7831–7839.

Cao, L., Lin, Z., Peng, F., Wang, W., Huang, R., Wang, C., Yan, J., Liang, J., Zhang, Z., Zhang, T., Long, L., Sun, J., Lin, W., 2016. Self-supporting metal–organic layers as single-site solid catalysts. Angew. Chem. Int. Ed. 55 (16), 4962–4966.

Chen, D., Li, B., Jiang, L., Duan, D., Li, Y., Wang, J., He, J., Zeng, Y., 2015. Highly efficient colorimetric detection of cancer cells utilizing Fe-MIL-101 with intrinsic peroxidase-like catalytic activity over a broad pH range. RSC Adv. 5 (119), 97910–97917.

Chen, F.-F., Zhu, Y.-J., Xiong, Z.-C., Sun, T.-W., 2017a. Hydroxyapatite Nanowires@ Metal–organic framework core/shell nanofibers: templated synthesis, peroxidase-like activity, and derived flexible recyclable test paper. Chem. Eur J. 23 (14), 3328–3337.

Chen, H., Qiu, Q., Sharif, S., Ying, S., Wang, Y., Ying, Y., 2018a. Solution-phase synthesis of platinum nanoparticle-decorated metal-organic framework hybrid nanomaterials as biomimetic nanoenzymes for biosensing applications. ACS Appl. Mater. Interfaces 10 (28), 24108–24115.

Chen, H., Yang, T., Liu, F., Li, W., 2018b. Electrodeposition of gold nanoparticles on Cu-based metal-organic framework for the electrochemical detection of nitrite. Sens. Actuators, B 286, 401–407.

Chen, J., Shu, Y., Li, H., Xu, Q., Hu, X., 2018c. Nickel metal-organic framework 2D nanosheets with enhanced peroxidase nanozyme activity for colorimetric detection of H$_2$O$_2$. Talanta 189, 254–261.

Chen, J., Xu, Q., Shu, Y., Hu, X., 2018d. Synthesis of a novel Au nanoparticles decorated Ni-MOF/Ni/NiO nanocomposite and electrocatalytic performance for the detection of glucose in human serum. Talanta 184, 136–142.

Chen, K., Wu, C.-D., 2018. Designed fabrication of biomimetic metal–organic frameworks for catalytic applications. Coord. Chem. Rev. 378, 445–465.

Chen, L., Xu, S., Li, J., 2011. Recent advances in molecular imprinting technology: current status, challenges and highlighted applications. Chem. Soc. Rev. 40 (5), 2922–2942.

Chen, Q., Xu, M., Zheng, W., Xu, T., Deng, H., Liu, J., 2017b. Se/Ru-Decorated porous metal–organic framework nanoparticles for the delivery of pooled siRNAs to reversing multidrug resistance in taxol-resistant breast cancer cells. ACS Appl. Mater. Interfaces 9 (8), 6712–6724.

Chen, W.-H., Luo, G.-F., Vázquez-González, M., Cazelles, R., Sohn, Y.S., Nechushtai, R., Mandel, I., Willner, I., 2018e. Glucose-responsive metal–organic-framework nanoparticles act as "smart" sense-and-treat carriers. ACS Nano 12 (8), 7538–7545.

Chen, W.-H., Vázquez-González, M., Kozell, A., Cecconello, A., Willner, I., 2018f. Cu2 + -Modified metal–organic framework nanoparticles: a peroxidase-mimicking nanoenzyme. Small 14 (5), 1703149.

Chen, X., Pradhan, T., Wang, F., Kim, J.S., Yoon, J., 2012. Fluorescent chemosensors based on spiroring-opening of xanthenes and related derivatives. Chem. Rev. 112 (3), 1910–1956.

Chen, Y.-Z., Zhang, R., Jiao, L., Jiang, H.-L., 2018g. Metal–organic framework-derived porous materials for catalysis. Coord. Chem. Rev. 362, 1–23.

Chen, Y., Xianyu, Y., Dong, M., Zhang, J., Zheng, W., Qian, Z., Jiang, X., 2018h. Cascade reaction-mediated assembly of magnetic/silver nanoparticles for amplified magnetic biosensing. Anal. Chem. 90 (11), 6906–6912.

Chen, Y., Xianyu, Y., Wu, J., Dong, M., Zheng, W., Sun, J., Jiang, X., 2017c. Double-enzymes-mediated bioluminescent sensor for quantitative and ultrasensitive point-of-care testing. Anal. Chem. 89 (10), 5422–5427.

Cheng, H., Liu, Y., Hu, Y., Ding, Y., Lin, S., Cao, W., Wang, Q., Wu, J., Muhammad, F., Zhao, X., Zhao, D., Li, Z., Xing, H., Wei, H., 2017. Monitoring of heparin activity in live rats using metal–organic framework nanosheets as peroxidase mimics. Anal. Chem. 89 (21), 11552–11559.

Cheng, H., Zhang, L., He, J., Guo, W., Zhou, Z., Zhang, X., Nie, S., Wei, H., 2016. Integrated nanozymes with nanoscale proximity for in vivo neurochemical monitoring in living brains. Anal. Chem. 88 (10), 5489–5497.

Cohen, S.M., 2017. The postsynthetic renaissance in porous solids. J. Am. Chem. Soc. 139 (8), 2855–2863.

Cui, F., Deng, Q., Sun, L., 2015a. Prussian blue modified metal–organic framework MIL-101 (Fe) with intrinsic peroxidase-like catalytic activity as a colorimetric biosensing platform. RSC Adv. 5 (119), 98215–98221.

Cui, F., Deng, Q., Sun, L., 2015b. Prussian blue modified metal–organic framework MIL-101(Fe) with intrinsic peroxidase-like catalytic activity as a colorimetric biosensing platform. RSC Adv. 5 (119), 98215–98221.

Cui, Y., Rimoldi, M., Platero-Prats, A.E., Chapman, K.W., Hupp, J.T., Farha, O.K., 2018. Stabilizing a vanadium oxide catalyst by supporting on a metal–organic framework. ChemCatChem 10 (8), 1772–1777.

Dalapati, R., Sakthivel, B., Ghosalya, M.K., Dhakshinamoorthy, A., Biswas, S., 2017. A cerium-based metal–organic framework having inherent oxidase-like activity applicable for colorimetric sensing of biothiols and aerobic oxidation of thiols. CrystEngComm 19 (39), 5915–5925.

Deng, H., Doonan, C.J., Furukawa, H., Ferreira, R.B., Towne, J., Knobler, C.B., Wang, B., Yaghi, O.M., 2010. Multiple functional groups of varying ratios in metal-organic frameworks. Science 327 (5967), 846–850.

Dinda, S., Sarkar, S., Das, P.K., 2018. Glucose oxidase mediated targeted cancer-starving therapy by biotinylated self-assembled vesicles. Chem. Commun. 54 (71), 9929–9932.

Dong, W., Yang, L., Huang, Y., 2017a. Glycine post-synthetic modification of MIL-53 (Fe) metal–organic framework with enhanced and stable peroxidase-like activity for sensitive glucose biosensing. Talanta 167, 359–366.

Dong, W., Yang, L., Huang, Y., 2017b. Glycine post-synthetic modification of MIL-53(Fe) metal–organic framework with enhanced and stable peroxidase-like activity for sensitive glucose biosensing. Talanta 167, 359–366.

Dong, W., Zhuang, Y., Li, S., Zhang, X., Chai, H., Huang, Y., 2018. High peroxidase-like activity of metallic cobalt nanoparticles encapsulated in metal–organic frameworks derived carbon for biosensing. Sens. Actuators, B 255, 2050–2057.

Fan, K., Wang, H., Xi, J., Liu, Q., Meng, X., Duan, D., Gao, L., Yan, X., 2017. Optimization of Fe 3 O 4 nanozyme activity via single amino acid modification mimicking an enzyme active site. Chem. Commun. 53 (2), 424–427.

Fan, L., Lou, D., Wu, H., Zhang, X., Zhu, Y., Gu, N., Zhang, Y., 2018. A novel AuNP-based glucose oxidase mimic with enhanced activity and selectivity constructed by molecular imprinting and O2-containing nanoemulsion embedding. Adv. Mater. Interfaces 5 (22), 1801070.

Farka, Z., Čunderlová, V., Horáčková, V., Pastucha, M., Mikušová, Z., Hlaváček, A., Skládal, P., 2018. Prussian blue nanoparticles as a catalytic label in a sandwich nanozyme-linked immunosorbent assay. Anal. Chem. 90 (3), 2348–2354.

Feng, D., Lei, T., Lukatskaya, M.R., Park, J., Huang, Z., Lee, M., Shaw, L., Chen, S., Yakovenko, A.A., Kulkarni, A., Xiao, J., Fredrickson, K., Tok, J.B., Zou, X., Cui, Y., Bao, Z., 2018. Robust and conductive two-dimensional metal − organic frameworks with exceptionally high volumetric and areal capacitance. Nat. Energy 3 (1), 30–36.

Fu, L.-H., Qi, C., Lin, J., Huang, P., 2018. Catalytic chemistry of glucose oxidase in cancer diagnosis and treatment. Chem. Soc. Rev. 47 (17), 6454–6472.

Gao, C., Zhu, H., Chen, J., Qiu, H., 2017a. Facile synthesis of enzyme functional metal-organic framework for colorimetric detecting H$_2$O$_2$ and ascorbic acid. Chin. Chem. Lett. 28 (5), 1006–1012.

Gao, L., Ju, L., Cui, H., 2017b. Chemiluminescent and fluorescent dual-signal graphene quantum dots and their application in pesticide sensing arrays. J. Mater. Chem. C 5 (31), 7753–7758.

Gao, L., Yan, X., 2016. Nanozymes: an emerging field bridging nanotechnology and biology. Sci. China Life Sci. 59 (4), 400–402.

Gao, L., Zhuang, J., Nie, L., Zhang, J., Zhang, Y., Gu, N., Wang, T., Feng, J., Yang, D., Perrett, S., Yan, X., 2007. Intrinsic peroxidase-like activity of ferromagnetic nanoparticles. Nat. Nanotechnol. 2, 577.

Gao, X., Wang, Y., Ji, G., Cui, R., Liu, Z., 2018. One-pot synthesis of hierarchical-pore metal–organic frameworks for drug delivery and fluorescent imaging. CrystEngComm 20 (8), 1087–1093.

Guan, Q., Li, Y.-A., Li, W.-Y., Dong, Y.-B., 2018. Photodynamic therapy based on nanoscale metal–organic frameworks: from material design to cancer nanotherapeutics. Chem. Asian J. 13 (21), 3122–3149.

Hartshorn, C.M., Bradbury, M.S., Lanza, G.M., Nel, A.E., Rao, J., Wang, A.Z., Wiesner, U.B., Yang, L., Grodzinski, P., 2018. Nanotechnology strategies to advance outcomes in clinical cancer care. ACS Nano 12 (1), 24–43.

He, J., Zhang, Y., Zhang, X., Huang, Y., 2018a. Highly efficient Fenton and enzyme-mimetic activities of NH2-MIL-88B(Fe) metal organic framework for methylene blue degradation. Sci. Rep. 8 (1), 5159.

He, T., Ni, B., Zhang, S., Gong, Y., Wang, H., Gu, L., Zhuang, J., Hu, W., Wang, X., 2018b. Ultrathin 2D zirconium metal–organic framework nanosheets: preparation and application in photocatalysis. Small 14 (16), 1703929.

Homaei, A.A., Sariri, R., Vianello, F., Stevanato, R., 2013. Enzyme immobilization: an update. J. Chem. Biol. 6 (4), 185–205.

Hou, C., Zhao, D., Wang, Y., Zhang, S., Li, S., 2018. Preparation of magnetic Fe3O4/PPy@ ZIF-8 nanocomposite for glucose oxidase immobilization and used as glucose electrochemical biosensor. J. Electroanal. Chem. 822, 50–56.

Hu, M., Lou, H., Yan, X., Hu, X., Feng, R., Zhou, M., 2018a. In-situ fabrication of ZIF-8 decorated layered double oxides for adsorption and photocatalytic degradation of methylene blue. Microporous Mesoporous Mater. 271, 68–72.

Hu, S., Yan, J., Huang, X., Guo, L., Lin, Z., Luo, F., Qiu, B., Wong, K.-Y., Chen, G., 2018b. A sensing platform for hypoxanthine detection based on amino-functionalized metal organic framework nanosheet with peroxidase mimic and fluorescence properties. Sens. Actuators, B 267, 312–319.

Hu, S., Zhu, L., Lam, C.W., Guo, L., Lin, Z., Qiu, B., Wong, K.Y., Chen, G., Liu, Z., 2019. Fluorometric determination of the activity of inorganic pyrophosphatase and its inhibitors by exploiting the peroxidase mimicking properties of a two-dimensional metal organic framework. Microchim. Acta 186 (3), 190.

Hu, Y., Cheng, H., Zhao, X., Wu, J., Muhammad, F., Lin, S., He, J., Zhou, L., Zhang, C., Deng, Y., 2017a. Surface-enhanced Raman scattering active gold nanoparticles with enzyme-mimicking activities for measuring glucose and lactate in living tissues. ACS Nano 11 (6), 5558–5566.

Hu, Y., Cheng, H., Zhao, X., Wu, J., Muhammad, F., Lin, S., He, J., Zhou, L., Zhang, C., Deng, Y., Wang, P., Zhou, Z., Nie, S., Wei, H., 2017b. Surface-enhanced Raman scattering active gold nanoparticles with enzyme-mimicking activities for measuring glucose and lactate in living tissues. ACS Nano 11 (6), 5558–5566.

Hu, Z., Jiang, X., Xu, F., Jia, J., Long, Z., Hou, X., 2016. Colorimetric sensing of bithiols using photocatalytic UiO-66(NH2) as H2O2-free peroxidase mimics. Talanta 158, 276–282.

Huang, L., Zhu, Q., Zhu, J., Luo, L., Pu, S., Zhang, W., Zhu, W., Sun, J., Wang, J., 2019a. Portable colorimetric detection of mercury (II) based on a non-noble metal nanozyme with tunable activity. Inorg. Chem. 58 (2), 1638–1646.

Huang, Y., Ren, J., Qu, X., 2019b. Nanozymes: classification, catalytic mechanisms, activity regulation, and applications. Chem. Rev. 119 (6), 4357–4412.

Huang, Y., Zhao, M., Han, S., Lai, Z., Yang, J., Tan, C., Ma, Q., Lu, Q., Chen, J., Zhang, X., 2017a. Growth of Au nanoparticles on 2D metalloporphyrinic metal-organic framework nanosheets used as biomimetic catalysts for cascade reactions. Adv. Mater. 29 (32), 1700102.

Huang, Y., Zhao, M., Han, S., Lai, Z., Yang, J., Tan, C., Ma, Q., Lu, Q., Chen, J., Zhang, X., Zhang, Z., Li, B., Chen, B., Zong, Y., Zhang, H., 2017b. Growth of Au nanoparticles on 2D metalloporphyrinic metal-organic framework nanosheets used as biomimetic catalysts for cascade reactions. Adv. Mater. 29 (32), 1700102.

Huo, M., Wang, L., Chen, Y., Shi, J., 2017. Tumor-selective catalytic nanomedicine by nanocatalyst delivery. Nat. Commun. 8 (1), 357.

Huo, M., Wang, L., Wang, Y., Chen, Y., Shi, J., 2019. Nanocatalytic tumor therapy by single-atom catalysts. ACS Nano 13 (2), 2643–2653.

Jiang, Y., Sun, D.-W., Pu, H., Wei, Q., 2018. Surface enhanced Raman spectroscopy (SERS): a novel reliable technique for rapid detection of common harmful chemical residues. Trends Food Sci. Technol. 75, 10–22.

Jiang, Z., Gao, P., Yang, L., Huang, C., Li, Y., 2015. Facile in situ synthesis of silver nanoparticles on the surface of metal–organic framework for ultrasensitive surface-enhanced Raman scattering detection of dopamine. Anal. Chem. 87 (24), 12177–12182.

Jiang, Z.W., Dai, F.Q., Huang, C.Z., Li, Y.F., 2016. Facile synthesis of a Fe3O4/MIL-101(Fe) composite with enhanced catalytic performance. RSC Adv. 6 (89), 86443–86446.

Jiao, L., Wang, Y., Jiang, H.-L., Xu, Q., 2018. Metal–organic frameworks as platforms for catalytic applications. Adv. Mater. 30 (37), 1703663.

Kan, J.-L., Jiang, Y., Xue, A., Yu, Y.-H., Wang, Q., Zhou, Y., Dong, Y.-B., 2018. Surface decorated porphyrinic nanoscale metal–organic framework for photodynamic therapy. Inorg. Chem. 57 (9), 5420–5428.

Kempahanumakkagari, S., Kumar, V., Samaddar, P., Kumar, P., Ramakrishnappa, T., Kim, K.-H., 2018a. Biomolecule-embedded metal-organic frameworks as an innovative sensing platform. Biotechnol. Adv. 36 (2), 467–481.

Kempahanumakkagari, S., Vellingiri, K., Deep, A., Kwon, E.E., Bolan, N., Kim, K.-H., 2018b. Metal–organic framework composites as electrocatalysts for electrochemical sensing applications. Coord. Chem. Rev. 357, 105–129.

Kim, H.N., Ren, W.X., Kim, J.S., Yoon, J., 2012. Fluorescent and colorimetric sensors for detection of lead, cadmium, and mercury ions. Chem. Soc. Rev. 41 (8), 3210–3244.

Ko, M., Mendecki, L., Mirica, K.A., 2018. Conductive two-dimensional metal–organic frameworks as multifunctional materials. Chem. Commun. 54 (57), 7873–7891.

Kong, W., Zhao, X., Zhu, Q., Gao, L., Cui, H., 2017. Highly chemiluminescent magnetic beads for label-free sensing of 2,4,6-trinitrotoluene. Anal. Chem. 89 (13), 7145–7151.

Kreno, L.E., Leong, K., Farha, O.K., Allendorf, M., Van Duyne, R.P., Hupp, J.T., 2012. Metal–organic framework materials as chemical sensors. Chem. Rev. 112 (2), 1105–1125.

Kukkar, D., Vellingiri, K., Kim, K.-H., Deep, A., 2018. Recent progress in biological and chemical sensing by luminescent metal-organic frameworks. Sensor. Actuator. B Chem. 273, 1346–1370.

Lan, G., Ni, K., Lin, W., 2019. Nanoscale metal–organic frameworks for phototherapy of cancer. Coord. Chem. Rev. 379, 65–81.

Lan, G., Ni, K., Xu, R., Lu, K., Lin, Z., Chan, C., Lin, W., 2017. Nanoscale metal–organic layers for deeply penetrating X-ray-induced photodynamic therapy. Angew. Chem. 129 (40), 12270–12274.

Lan, G., Ni, K., Xu, Z., Veroneau, S.S., Song, Y., Lin, W., 2018. Nanoscale metal–organic framework overcomes hypoxia for photodynamic therapy primed cancer immunotherapy. J. Am. Chem. Soc. 140 (17), 5670–5673.

Lei, Z., Gao, C., Chen, L., He, Y., Ma, W., Lin, Z., 2018. Recent advances in biomolecule immobilization based on self-assembly: organic–inorganic hybrid nanoflowers and metal–organic frameworks as novel substrates. J. Mater. Chem. B 6 (11), 1581–1594.

Li, B., Chen, D., Wang, J., Yan, Z., Jiang, L., Duan, D., He, J., Luo, Z., Zhang, J., Yuan, F., 2014. MOFzyme: intrinsic protease-like activity of Cu-MOF. Sci. Rep. 4, 6759.

Li, D., Wu, S., Wang, F., Jia, S., Liu, Y., Han, X., Zhang, L., Zhang, S., Wu, Y., 2016a. A facile one-pot synthesis of hemin/ZIF-8 composite as mimetic peroxidase. Mater. Lett. 178, 48–51.

Li, H., Han, W., Lv, R., Zhai, A., Li, X.-L., Gu, W., Liu, X., 2019a. A dual-function mixed-lanthanide metal-organic framework for ratiometric water detection in bio-ethanol and temperature sensing. Anal. Chem. 91 (3), 2148–2154.

Li, J., Yan, X., Li, X., Zhang, X., Chen, J., 2018a. A new electrochemical immunosensor for sensitive detection of prion based on Prussian blue analogue. Talanta 179, 726–733.

Li, P., Moon, S.-Y., Guelta, M.A., Harvey, S.P., Hupp, J.T., Farha, O.K., 2016b. Encapsulation of a nerve agent detoxifying enzyme by a mesoporous zirconium metal–organic framework engenders thermal and long-term stability. J. Am. Chem. Soc. 138 (26), 8052–8055.

Li, S.-Y., Cheng, H., Xie, B.-R., Qiu, W.-X., Zeng, J.-Y., Li, C.-X., Wan, S.-S., Zhang, L., Liu, W.-L., Zhang, X.-Z., 2017a. Cancer cell membrane camouflaged cascade bioreactor for cancer targeted starvation and photodynamic therapy. ACS Nano 11 (7), 7006–7018.

Li, S., Liu, X., Chai, H., Huang, Y., 2018b. Recent advances in the construction and analytical applications of metal-organic frameworks-based nanozymes. TrAC Trends Anal. Chem. (Reference Ed.) 105, 391–403.

Li, S., Liu, X., Chai, H., Huang, Y., 2018c. Recent advances in the construction and analytical applications of metal-organic frameworks-based nanozymes. TrAC Trends Anal. Chem. (Reference Ed.) 105, 391–403.

Li, S., Wang, L., Zhang, X., Chai, H., Huang, Y., 2018d. A Co,N co-doped hierarchically porous carbon hybrid as a highly efficient oxidase mimetic for glutathione detection. Sens. Actuators, B 264, 312–319.

Li, W., Chen, B., Zhang, H., Sun, Y., Wang, J., Zhang, J., Fu, Y., 2015. BSA-stabilized Pt nanozyme for peroxidase mimetics and its application on colorimetric detection of mercury(II) ions. Biosens. Bioelectron. 66, 251–258.

Li, X., Zhang, H., Tang, Y., Wu, P., Xu, S., Zhang, X., 2017b. A both-end blocked peroxidase-mimicking DNAzyme for low-background chemiluminescent sensing of miRNA. ACS Sens. 2 (6), 810–816.

Li, Y., Wang, Z., Sun, L., Liu, L., Xu, C., Kuang, H., 2019b. Nanoparticle-based sensors for food contaminants. TrAC Trends Anal. Chem. (Reference Ed.) 113, 74–83.

Li, Y., You, S., Shi, X., 2017c. Enhanced chemiluminescence determination of hydrogen peroxide in milk sample using metal–organic framework Fe–MIL–88NH2 as peroxidase mimetic. Food Anal. Method. 10 (3), 626–633.

Li, Y., Xu, C., Yang, B., Liu, Z., Xia, P., Wang, Q., 2018e. Target-catalyzed hairpin assembly and metal-organic frameworks mediated nonenzymatic co-reaction for multiple signal amplification detection of miR-122 in human serum. Biosens. Bioelectron. 102, 307–315.

Lian, X., Fang, Y., Joseph, E., Wang, Q., Li, J., Banerjee, S., Lollar, C., Wang, X., Zhou, H.-C., 2017. Enzyme–MOF (metal–organic framework) composites. Chem. Soc. Rev. 46 (11), 3386–3401.

Liang, H., Lin, F., Zhang, Z., Liu, B., Jiang, S., Yuan, Q., Liu, J., 2017. Multicopper laccase mimicking nanozymes with nucleotides as ligands. ACS Appl. Mater. Interfaces 9 (2), 1352–1360.

Liang, W., Xu, H., Carraro, F., Maddigan, N.K., Li, Q., Bell, S.G., Huang, D.M., Tarzia, A., Solomon, M.B., Amenitsch, H., Vaccari, L., Sumby, C.J., Falcaro, P., Doonan, C.J., 2019. Enhanced activity of enzymes encapsulated in hydrophilic metal–organic frameworks. J. Am. Chem. Soc. 141 (6), 2348–2355.

Liang, Y., Shang, R., Lu, J., Liu, L., Hu, J., Cui, W., 2018a. Ag3PO4@ UMOFNs core–shell structure: two-dimensional MOFs promoted photoinduced charge separation and photocatalysis. ACS Appl. Mater. Interfaces 10 (10), 8758–8769.

Liang, Y., Shang, R., Lu, J., Liu, L., Hu, J., Cui, W., 2018b. Ag3PO4@UMOFNs core–shell structure: two-dimensional MOFs promoted photoinduced charge separation and photocatalysis. ACS Appl. Mater. Interfaces 10 (10), 8758–8769.

Liang, Z., Qu, C., Guo, W., Zou, R., Xu, Q., 2018c. Pristine metal–organic frameworks and their composites for energy storage and conversion. Adv. Mater. 30 (37), 1702891.

Lin, H., Chen, Y., Shi, J., 2018a. Nanoparticle-triggered in situ catalytic chemical reactions for tumour-specific therapy. Chem. Soc. Rev. 47 (6), 1938–1958.

Lin, T., Qin, Y., Huang, Y., Yang, R., Hou, L., Ye, F., Zhao, S., 2018b. A label-free fluorescence assay for hydrogen peroxide and glucose based on the bifunctional MIL-53(Fe) nanozyme. Chem. Commun. 54 (14), 1762–1765.

Ling, P., Qian, C., Gao, F., Lei, J., 2018. Enzyme-immobilized metal–organic framework nanosheets as tandem catalysts for the generation of nitric oxide. Chem. Commun. 54 (79), 11176–11179.

Liu, C., Luo, L., Zeng, L., Xing, J., Xia, Y., Sun, S., Zhang, L., Yu, Z., Yao, J., Yu, Z., Akakuru, O.U., Saeed, M., Wu, A., 2018a. Porous gold nanoshells on functional NH2-MOFs: facile synthesis and designable platforms for cancer multiple therapy. Small 14 (35), 1801851.

Liu, H., Ma, H., Xu, H., Wen, J., Huang, Z., Qiu, Y., Fan, K., Li, D., Gu, C., 2019a. Hollow and porous nickel sulfide nanocubes prepared from a metal-organic framework as an efficient enzyme mimic for colorimetric detection of hydrogen peroxide. Anal. Bioanal. Chem. 411 (1), 129–137.

Liu, L., Zhou, Y., Liu, S., Xu, M., 2018b. The applications of Metal−Organic frameworks in electrochemical sensors. ChemElectroChem 5 (1), 6–19.

Liu, M., Wang, L., Zheng, X., Liu, S., Xie, Z., 2018c. Hypoxia-triggered nanoscale metal–organic frameworks for enhanced anticancer activity. ACS Appl. Mater. Interfaces 10 (29), 24638–24647.

Liu, M., Zheng, W., Ran, S., Boles, S.T., Lee, L.Y.S., 2018e. Overall water-splitting electrocatalysts based on 2D CoNi-Metal-Organic frameworks and its derivative. Adv. Mater. Interfaces 0 (0), 1800849.

Liu, T.-Z., Hu, R., Zhang, X., Zhang, K.-L., Liu, Y., Zhang, X.-B., Bai, R.-Y., Li, D., Yang, Y.-H., 2016. Metal–organic framework nanomaterials as novel signal probes for electron transfer mediated ultrasensitive electrochemical immunoassay. Anal. Chem. 88 (24), 12516–12523.

Liu, W., Yin, X.-B., 2016. Metal–organic frameworks for electrochemical applications. TrAC Trends Anal. Chem. (Reference Ed.) 75, 86–96.

Liu, X., Qi, W., Wang, Y., Lin, D., Yang, X., Su, R., He, Z., 2018d. Rational design of mimic multienzyme systems in hierarchically porous biomimetic metal–organic frameworks. ACS Appl. Mater. Interfaces 10 (39), 33407–33415.

Liu, X., Qi, W., Wang, Y., Su, R., He, Z., 2018e. Exploration of intrinsic lipase-like activity of zirconium-based metal-organic frameworks. Eur. J. Inorg. Chem. (41), 4579–4585 2018.

Liu, Y., Li, H., Lu, L., Sun, B., Huang, L., Chen, H., Qiu, W., Tao, J., Zhao, P., 2019b. A ratiometric electrochemical sensor with integrated probe for the assay of α-glucosidase activity and screening of its inhibitors. J. Electrochem. Soc. 166 (2), B133–B140.

Liu, Y.L., Zhao, X.J., Yang, X.X., Li, Y.F., 2013. A nanosized metal–organic framework of Fe-MIL-88NH2 as a novel peroxidase mimic used for colorimetric detection of glucose. Analyst 138 (16), 4526–4531.

Lu, J., Xiong, Y., Liao, C., Ye, F., 2015. Colorimetric detection of uric acid in human urine and serum based on peroxidase mimetic activity of MIL-53 (Fe). Anal. Methods 7 (23), 9894–9899.

Lu, K., Aung, T., Guo, N., Weichselbaum, R., Lin, W., 2018a. Nanoscale metal–organic frameworks for therapeutic, imaging, and sensing applications. Adv. Mater. 30 (37), 1707634.

Lu, K., He, C., Guo, N., Chan, C., Ni, K., Lan, G., Tang, H., Pelizzari, C., Fu, Y.-X., Spiotto, M.T., 2018b. Low-dose X-ray radiotherapy–radiodynamic therapy via nanoscale metal–organic frameworks enhances checkpoint blockade immunotherapy. Nature Biomedical Engineering 1.

Luo, F., Lin, Y., Zheng, L., Lin, X., Chi, Y., 2015. Encapsulation of hemin in metal–organic frameworks for catalyzing the chemiluminescence reaction of the H2O2–luminol system and detecting glucose in the neutral condition. ACS Appl. Mater. Interfaces 7 (21), 11322–11329.

Ma, C., Ma, Y., Sun, Y., Lu, Y., Tian, E., Lan, J., Li, J., Ye, W., Zhang, H., 2019. Colorimetric determination of Hg2 + in environmental water based on the Hg2 + -stimulated peroxidase mimetic activity of MoS2-Au composites. J. Colloid Interface Sci. 537, 554–561.

Ma, M., Wen, K., Beier, R.C., Eremin, S.A., Li, C., Zhang, S., Shen, J., Wang, Z., 2016. Chemiluminescence resonance energy transfer competitive immunoassay employing hapten-functionalized quantum dots for the detection of sulfamethazine. ACS Appl. Mater. Interfaces 8 (28), 17745–17750.

Ma, X., Wen, S., Xue, X., Guo, Y., Jin, J., Song, W., Zhao, B., 2018. Controllable synthesis of SERS-active magnetic metal–organic framework-based nanocatalysts and their application in photoinduced enhanced catalytic oxidation. ACS Appl. Mater. Interfaces 10 (30), 25726–25736.

Majdinasab, M., Mitsubayashi, K., Marty, J.L., 2019. Optical and electrochemical sensors and biosensors for the detection of quinolones. Trends Biotechnol. https://doi.org/10.1016/j.tibtech.2019.01.004.

Mao, X., Lu, Y., Zhang, X., Huang, Y., 2018. β-Cyclodextrin functionalization of metal-organic framework MOF-235 with excellent chemiluminescence activity for sensitive glucose biosensing. Talanta 188, 161–167.

Mehta, J., Bhardwaj, N., Bhardwaj, S.K., Kim, K.-H., Deep, A., 2016. Recent advances in enzyme immobilization techniques: metal-organic frameworks as novel substrates. Coord. Chem. Rev. 322, 30–40.

Meng, W., Wen, Y., Dai, L., He, Z., Wang, L., 2018. A novel electrochemical sensor for glucose detection based on Ag@ZIF-67 nanocomposite. Sens. Actuators, B 260, 852–860.

Menon, S.S., Chandran, S.V., Koyappayil, A., Berchmans, S., 2018. Copper- based metal-organic frameworks as peroxidase mimics leading to sensitive $H_2O_2$ and glucose detection. Chemistry 3 (28), 8319–8324.

Michopoulos, A., Kouloumpis, A., Gournis, D., Prodromidis, M.I., 2014. Performance of layer-by-layer deposited low dimensional building blocks of graphene-prussian blue onto graphite screen-printed electrodes as sensors for hydrogen peroxide. Electrochim. Acta 146, 477–484.

Morozan, A., Jaouen, F., 2012. Metal organic frameworks for electrochemical applications. Energy Environ. Sci. 5 (11), 9269–9290.

Nguyen, V.D., Nguyen, C.K., Tran, K.N., Tu, T.N., Nguyen, T.T., Dang, H.V., Truong, T., Phan, N.T.S., 2018. Zeolite imidazolate frameworks in catalysis: synthesis of benzimidazoles via cascade redox condensation using Co-ZIF-67 as an efficient heterogeneous catalyst. Appl. Catal. Gen. 555, 20–26.

Ni, K., Lan, G., Veroneau, S.S., Duan, X., Song, Y., Lin, W., 2018. Nanoscale metal-organic frameworks for mitochondria-targeted radiotherapy-radiodynamic therapy. Nat. Commun. 9 (1), 4321.

Pham, X.-H., Hahm, E., Kim, T.H., Kim, H.-M., Lee, S.H., Lee, Y.-S., Jeong, D.H., Jun, B.-H., 2018. Enzyme-catalyzed Ag growth on Au nanoparticle-assembled structure for highly sensitive colorimetric immunoassay. Sci. Rep. 8 (1), 6290.

Phan, L.M.T., Rafique, R., Baek, S.H., Nguyen, T.P., Park, K.Y., Kim, E.B., Kim, J.G., Park, J.P., Kailasa, S.K., Kim, H.-J., Chung, C., Shim, T.S., Park, T.J., 2018. Gold-copper nanoshell dot-blot immunoassay for naked-eye sensitive detection of tuberculosis specific CFP-10 antigen. Biosens. Bioelectron. 121, 111–117.

Qian Tang, X., Dan Zhang, Y., Wei Jiang, Z., Mei Wang, D., Zhi Huang, C., Fang Li, Y., 2018. Fe3O4 and metal–organic framework MIL-101(Fe) composites catalyze luminol chemiluminescence for sensitively sensing hydrogen peroxide and glucose. Talanta 179, 43–50.

Qian, Y., Khan, I.A., Zhao, D., 2017. Electrocatalysts derived from metal–organic frameworks for oxygen reduction and evolution reactions in aqueous media. Small 13 (37), 1701143.

Qin, F.-X., Jia, S.-Y., Wang, F.-F., Wu, S.-H., Song, J., Liu, Y., 2013. Hemin@metal–organic framework with peroxidase-like activity and its application to glucose detection. Catalysis Science & Technology 3 (10), 2761–2768.

Qin, J., Wang, S., Wang, X., 2017. Visible-light reduction $CO_2$ with dodecahedral zeolitic imidazolate framework ZIF-67 as an efficient co-catalyst. Appl. Catal. B Environ. 209, 476–482.

Qin, L., Wang, X., Liu, Y., Wei, H., 2018. 2D-Metal–Organic-Framework-Nanozyme sensor arrays for probing phosphates and their enzymatic hydrolysis. Anal. Chem. 90 (16), 9983–9989.

Rajendrakumar, S.K., Uthaman, S., Cho, C.-S., Park, I.-K., 2018. Nanoparticle-based phototriggered cancer immunotherapy and its domino effect in the tumor microenvironment. Biomacromolecules 19 (6), 1869–1887.

Ren, R., Cai, G., Yu, Z., Zeng, Y., Tang, D., 2018. Metal-polydopamine framework: an innovative signal-generation tag for colorimetric immunoassay. Anal. Chem. 90 (18), 11099–11105.

Rojas, S., Baati, T., Njim, L., Manchego, L., Neffati, F., Abdeljelil, N., Saguem, S., Serre, C., Najjar, M.F., Zakhama, A., Horcajada, P., 2018. Metal–organic frameworks as efficient oral detoxifying agents. J. Am. Chem. Soc. 140 (30), 9581–9586.

Sadeghi, A.S., Ansari, N., Ramezani, M., Abnous, K., Mohsenzadeh, M., Taghdisi, S.M., Alibolandi, M., 2018. Optical and electrochemical aptasensors for the detection of amphenicols. Biosens. Bioelectron. 118, 137–152.

Shen, W.-J., Zhuo, Y., Chai, Y.-Q., Yuan, R., 2016. Ce-based metal-organic frameworks and DNAzyme-assisted recycling as dual signal amplifiers for sensitive electrochemical detection of lipopolysaccharide. Biosens. Bioelectron. 83, 287–292.

Song, F., Hu, X., 2014. Exfoliation of layered double hydroxides for enhanced oxygen evolution catalysis. Nat. Commun. 5, 4477.

Song, Y., Cho, D., Venkateswarlu, S., Yoon, M., 2017. Systematic study on preparation of copper nanoparticle embedded porous carbon by carbonization of metal–organic framework for enzymatic glucose sensor. RSC Adv. 7 (17), 10592–10600.

Su, L., Xiong, Y., Yang, H., Zhang, P., Ye, F., 2016. Prussian blue nanoparticles encapsulated inside a metal–organic framework via in situ growth as promising peroxidase mimetics for enzyme inhibitor screening. J. Mater. Chem. B 4 (1), 128–134.

Tan, B., Zhao, H., Wu, W., Liu, X., Zhang, Y., Quan, X., 2017a. Fe3O4-AuNPs anchored 2D metal–organic framework nanosheets with DNA regulated switchable peroxidase-like activity. Nanoscale 9 (47), 18699–18710.

Tan, C., Cao, X., Wu, X.-J., He, Q., Yang, J., Zhang, X., Chen, J., Zhao, W., Han, S., Nam, G.-H., Sindoro, M., Zhang, H., 2017b. Recent advances in ultrathin two-dimensional nanomaterials. Chem. Rev. 117 (9), 6225–6331.

Tan, D.C.L., Sato, H., 2017. Enhancing catalytic activity of bioanode for glucose biofuel cell by compressing enzyme, mediator and carbon support through centrifugation. Chem. Eur J. 23 (48), 11485–11488.

Tan, H., Li, Q., Zhou, Z., Ma, C., Song, Y., Xu, F., Wang, L., 2015. A sensitive fluorescent assay for thiamine based on metal-organic frameworks with intrinsic peroxidase-like activity. Anal. Chim. Acta 856, 90–95.

Tan, H., Ma, C., Gao, L., Li, Q., Song, Y., Xu, F., Wang, T., Wang, L., 2014. Metal–organic framework-derived copper Nanoparticle@Carbon nanocomposites as peroxidase mimics for colorimetric sensing of ascorbic acid. Chem. Eur J. 20 (49), 16377–16383.

Tang, L., Li, J., 2017. Plasmon-based colorimetric nanosensors for ultrasensitive molecular diagnostics. ACS Sens. 2 (7), 857–875.

Valekar, A.H., Batule, B.S., Kim, M.I., Cho, K.-H., Hong, D.-Y., Lee, U.H., Chang, J.-S., Park, H.G., Hwang, Y.K., 2018. Novel amine-functionalized iron trimesates with enhanced peroxidase-like activity and their applications for the fluorescent assay of choline and acetylcholine. Biosens. Bioelectron. 100, 161–168.

Vermoortele, F., Bueken, B., Le Bars, G., Van de Voorde, B., Vandichel, M., Houthoofd, K., Vimont, A., Daturi, M., Waroquier, M., Van Speybroeck, V., Kirschhock, C., De Vos, D.E., 2013. Synthesis modulation as a tool to increase the catalytic activity of metal–organic frameworks: the unique case of UiO-66(Zr). J. Am. Chem. Soc. 135 (31), 11465–11468.

Vo, Y.H., Le, T.V., Nguyen, H.D., To, T.A., Ha, H.Q., Nguyen, A.T., Phan, A.N., Phan, N.T., 2018. Synthesis of quinazolinones and benzazoles utilizing recyclable sulfated metal-organic framework-808 catalyst in glycerol as green solvent. J. Ind. Eng. Chem. 64, 107–115.

Wang, C., Gao, J., Cao, Y., Tan, H., 2018a. Colorimetric logic gate for alkaline phosphatase based on copper (II)-based metal-organic frameworks with peroxidase-like activity. Anal. Chim. Acta 1004, 74–81.

Wang, C., Gao, J., Tan, H., 2018b. Integrated antibody with catalytic metal–organic framework for colorimetric immunoassay. ACS Appl. Mater. Interfaces 10 (30), 25113–25120.

Wang, C., Tang, G., Tan, H., 2018c. Colorimetric determination of mercury(II) via the inhibition by ssDNA of the oxidase-like activity of a mixed valence state cerium-based metal-organic framework. Microchim. Acta 185 (10), 475.

Wang, C., Xie, Z., deKrafft, K.E., Lin, W., 2011. Doping metal–organic frameworks for water oxidation, carbon dioxide reduction, and organic photocatalysis. J. Am. Chem. Soc. 133 (34), 13445–13454.

Wang, H.-S., 2017. Metal–organic frameworks for biosensing and bioimaging applications. Coord. Chem. Rev. 349, 139–155.

Wang, S., Deng, W., Yang, L., Tan, Y., Xie, Q., Yao, S., 2017. Copper-based metal–organic framework nanoparticles with peroxidase-like activity for sensitive colorimetric detection of Staphylococcus aureus. ACS Appl. Mater. Interfaces 9 (29), 24440–24445.

Wang, X., Qin, L., Zhou, M., Lou, Z., Wei, H., 2018d. Nanozyme sensor arrays for detecting versatile analytes from small molecules to proteins and cells. Anal. Chem. 90 (19), 11696–11702.

Wang, Y., Zhao, M., Ping, J., Chen, B., Cao, X., Huang, Y., Tan, C., Ma, Q., Wu, S., Yu, Y., Lu, Q., Chen, J., Zhao, W., Ying, Y., Zhang, H., 2016b. Bioinspired design of ultrathin 2D bimetallic metal–organic-framework nanosheets used as biomimetic enzymes. Adv. Mater. 28 (21), 4149–4155.

Wang, Y., Zhu, Y., Binyam, A., Liu, M., Wu, Y., Li, F., 2016c. Discovering the enzyme mimetic activity of metal-organic framework (MOF) for label-free and colorimetric sensing of biomolecules. Biosens. Bioelectron. 86, 432–438.

Wei, H., Wang, E.K., 2013. Nanomaterials with enzyme-like characteristics (nanozymes): next-generation artificial enzymes. Chem. Soc. Rev. 42 (14), 6060–6093.

Wei, X., Wang, S., Hua, Z., Chen, L., Shi, J., 2018. Metal–organic framework nanosheet electrocatalysts for efficient H2 production from methanol solution: methanol-assisted water splitting or methanol reforming? ACS Appl. Mater. Interfaces 10 (30), 25422–25428.

Wu, D., Hu, N., Liu, J., Fan, G., Li, X., Sun, J., Dai, C., Suo, Y., Li, G., Wu, Y., 2018a. Ultrasensitive colorimetric sensing strategy based on ascorbic acid triggered remarkable photoactive-nanoperoxidase for signal amplification and its application to α-glucosidase activity detection. Talanta 190, 103–109.

Wu, J., Chen, Y., Yang, M., Wang, Y., Zhang, C., Yang, M., Sun, J., Xie, M., Jiang, X., 2017a. Streptavidin-biotin-peroxidase nanocomplex-amplified microfluidics immunoassays for simultaneous detection of inflammatory biomarkers. Anal. Chim. Acta 982, 138–147.

Wu, J., Li, S., Wei, H., 2018b. Integrated nanozymes: facile preparation and biomedical applications. Chem. Commun. 54 (50), 6520–6530.

Wu, J., Wang, X., Wang, Q., Lou, Z., Li, S., Zhu, Y., Qin, L., Wei, H., 2019. Nanomaterials with enzyme-like characteristics (nanozymes): next-generation artificial enzymes (II). Chem. Soc. Rev. 48 (4), 1004–1076.

Wu, M.-X., Yang, Y.-W., 2017. Metal–organic framework (MOF)-Based drug/cargo delivery and cancer therapy. Adv. Mater. 29 (23), 1606134.

Wu, Y., Ma, Y., Xu, G., Wei, F., Ma, Y., Song, Q., Wang, X., Tang, T., Song, Y., Shi, M., Xu, X., Hu, Q., 2017b. Metal-organic framework coated Fe3O4 magnetic nanoparticles with peroxidase-like activity for colorimetric sensing of cholesterol. Sens. Actuators, B 249, 195–202.

Xie, Y., Song, Y., Zhang, Y., Xu, L., Miao, L., Peng, C., Wang, L., 2018. Cu metal-organic framework-derived Cu Nanospheres@Porous carbon/macroporous carbon for electrochemical sensing glucose. J. Alloy. Comp. 757, 105–111.

Xiong, Y., Chen, S., Ye, F., Su, L., Zhang, C., Shen, S., Zhao, S., 2015. Synthesis of a mixed valence Ce-MOF as an oxidase mimetic for the colorimetric detection of biothiols. Chem. Commun. 51 (22), 4635–4638.

Xu, Y., Li, Q., Xue, H., Pang, H., 2018. Metal-organic frameworks for direct electrochemical applications. Coord. Chem. Rev. 376, 292–318.

Yan, X., Zhao, Y., Yang, H., Kang, X.-J., Wang, L.-L., Lu, Z.-D., 2018. Ultrasmall Au nanoparticles embedded in 2D mixed-ligand metal–organic framework nanosheets exhibiting highly efficient and size-selective catalysis. Adv. Funct. Mater. 28 (34), 1802021.

Yang, H., Yang, R., Zhang, P., Qin, Y., Chen, T., Ye, F., 2017a. A bimetallic (Co/2Fe) metal-organic framework with oxidase and peroxidase mimicking activity for colorimetric detection of hydrogen peroxide. Microchim. Acta 184 (12), 4629–4635.

Yang, L., Xu, C., Ye, W., Liu, W., 2015. An electrochemical sensor for H2O2 based on a

new Co-metal-organic framework modified electrode. Sens. Actuators, B 215, 489–496.

Yang, Q., Xu, Q., Jiang, H.-L., 2017b. Metal–organic frameworks meet metal nanoparticles: synergistic effect for enhanced catalysis. Chem. Soc. Rev. 46 (15), 4774–4808.

Yang, X., Li, L., He, D., Hai, L., Tang, J., Li, H., He, X., Wang, K., 2017c. A metal–organic framework based nanocomposite with co-encapsulation of Pd@Au nanoparticles and doxorubicin for pH- and NIR-triggered synergistic chemo-photothermal treatment of cancer cells. J. Mater. Chem. B 5 (24), 4648–4659.

Yang, Y., Yang, Z., Lv, J., Yuan, R., Chai, Y., 2017d. Thrombin aptasensor enabled by Pt nanoparticles-functionalized Co-based metal organic frameworks assisted electrochemical signal amplification. Talanta 169, 44–49.

Ye, L., Gao, Y., Cao, S., Chen, H., Yao, Y., Hou, J., Sun, L., 2018. Assembly of highly efficient photocatalytic CO2 conversion systems with ultrathin two-dimensional metal–organic framework nanosheets. Appl. Catal. B Environ. 227, 54–60.

Yi, X., Dong, W., Zhang, X., Xie, J., Huang, Y., 2016a. MIL-53 (Fe) MOF-mediated catalytic chemiluminescence for sensitive detection of glucose. Anal. Bioanal. Chem. 408 (30), 8805–8812.

Yi, X., Dong, W., Zhang, X., Xie, J., Huang, Y., 2016b. MIL-53(Fe) MOF-mediated catalytic chemiluminescence for sensitive detection of glucose. Anal. Bioanal. Chem. 408 (30), 8805–8812.

Yin, B., Zheng, W., Dong, M., Yu, W., Chen, Y., Joo, S.W., Jiang, X., 2017. An enzyme-mediated competitive colorimetric sensor based on Au@Ag bimetallic nanoparticles for highly sensitive detection of disease biomarkers. Analyst 142 (16), 2954–2960.

Yin, M., Duan, Z., Zhang, C., Feng, L., Wan, Y., Cai, Y., Liu, H., Li, S., Wang, H., 2019. A visualized colorimetric detection strategy for heparin in serum using a metal-free polymer nanozyme. Microchem. J. 145, 864–871.

Yin, Y., Gao, C., Xiao, Q., Lin, G., Lin, Z., Cai, Z., Yang, H., 2016. Protein-metal organic framework hybrid composites with intrinsic peroxidase-like activity as a colorimetric biosensing platform. ACS Appl. Mater. Interfaces 8 (42), 29052–29061.

Zhai, M., Wang, F., Du, H., 2017. Transition-metal phosphide–carbon nanosheet composites derived from two-dimensional metal-organic frameworks for highly efficient electrocatalytic water-splitting. ACS Appl. Mater. Interfaces 9 (46), 40171–40179.

Zhang, C., Ni, D., Liu, Y., Yao, H., Bu, W., Shi, J., 2017a. Magnesium silicide nanoparticles as a deoxygenation agent for cancer starvation therapy. Nat. Nanotechnol. 12, 378.

Zhang, G.-Y., Zhuang, Y.-H., Shan, D., Su, G.-F., Cosnier, S., Zhang, X.-J., 2016. Zirconium-based porphyrinic metal–organic framework (PCN-222): enhanced photoelectrochemical response and its application for label-free phosphoprotein detection. Anal. Chem. 88 (22), 11207–11212.

Zhang, H., 2015. Ultrathin two-dimensional nanomaterials. ACS Nano 9 (10), 9451–9469.

Zhang, J.-W., Zhang, H.-T., Du, Z.-Y., Wang, X., Yu, S.-H., Jiang, H.-L., 2014. Water-stable metal–organic frameworks with intrinsic peroxidase-like activity as a colorimetric biosensing platform. Chem. Commun. 50 (9), 1092–1094.

Zhang, J., Zheng, W., Jiang, X., 2018a. Ag + -Gated surface chemistry of gold nanoparticles and colorimetric detection of acetylcholinesterase. Small 14 (31), 1801680.

Zhang, K., Meng, X., Cao, Y., Yang, Z., Dong, H., Zhang, Y., Lu, H., Shi, Z., Zhang, X., 2018b. Metal–organic framework nanoshuttle for synergistic photodynamic and low-temperature photothermal therapy. Adv. Funct. Mater. 28 (42), 1804634.

Zhang, K., Meng, X., Cao, Y., Yang, Z., Dong, H., Zhang, Y., Lu, H., Shi, Z., Zhang, X., 2018c. Metal–organic framework nanoshuttle for synergistic photodynamic and low-temperature photothermal therapy. Adv. Funct. Mater. 28 (42), 1804634.

Zhang, L., Fan, C., Liu, M., Liu, F., Bian, S., Du, S., Zhu, S., Wang, H., 2018d. Biomineralized gold-Hemin@MOF composites with peroxidase-like and gold catalysis activities: a high-throughput colorimetric immunoassay for alpha-fetoprotein in blood by ELISA and gold-catalytic silver staining. Sensor. Actuator. B Chem. 266, 543–552.

Zhang, L., Wang, Z., Zhang, Y., Cao, F., Dong, K., Ren, J., Qu, X., 2018e. Erythrocyte membrane cloaked metal–organic framework nanoparticle as biomimetic nanoreactor for starvation-activated colon cancer therapy. ACS Nano 12 (10), 10201–10211.

Zhang, W., Lu, J., Gao, X., Li, P., Zhang, W., Ma, Y., Wang, H., Tang, B., 2018g. Enhanced photodynamic therapy by reduced levels of intracellular glutathione obtained by employing a nano-MOF with CuII as the active center. Angew. Chem. 130 (18), 4985–4990.

Zhang, X., Chang, L., Yang, Z., Shi, Y., Long, C., Han, J., Zhang, B., Qiu, X., Li, G., Tang, Z., 2019. Facile synthesis of ultrathin metal-organic framework nanosheets for Lewis acid catalysis. Nano Research 12 (2), 437–440.

Zhang, Y., Su, K., Hao, M., Liu, L., Han, Z.-B., Yuan, D., 2018i. Two metal–organic frameworks based on pyridyl–tricarboxylate ligands as size-selective catalysts for solvent-free cyanosilylation reaction. CrystEngComm 20 (39), 6070–6076.

Zhang, Y., Wang, F., Liu, C., Wang, Z., Kang, L., Huang, Y., Dong, K., Ren, J., Qu, X., 2018j. Nanozyme decorated metal–organic frameworks for enhanced photodynamic therapy. ACS Nano 12 (1), 651–661.

Zhang, Y., Yuan, S., Day, G., Wang, X., Yang, X., Zhou, H.-C., 2018k. Luminescent sensors based on metal-organic frameworks. Coord. Chem. Rev. 354, 28–45.

Zhang, Z., Liu, B., Liu, J., 2017b. Molecular imprinting for substrate selectivity and enhanced activity of enzyme mimics. Small 13 (7).

Zhang, Z., Zhang, X., Liu, B., Liu, J., 2017c. Molecular imprinting on inorganic nanozymes for hundred-fold enzyme specificity. J. Am. Chem. Soc. 139 (15), 5412–5419.

Zhao, C., Jiang, Z., Mu, R., Li, Y., 2016. A novel sensor for dopamine based on the turn-on fluorescence of Fe-MIL-88 metal-organic frameworks–hydrogen peroxide–o-phenylenediamine system. Talanta 159, 365–370.

Zhao, M., Huang, Y., Peng, Y., Huang, Z., Ma, Q., Zhang, H., 2018b. Two-dimensional metal–organic framework nanosheets: synthesis and applications. Chem. Soc. Rev. 47 (16), 6267–6295.

Zhao, M., Wang, Y., Ma, Q., Huang, Y., Zhang, X., Ping, J., Zhang, Z., Lu, Q., Yu, Y., Xu, H., Zhao, Y., Zhang, H., 2015. Ultrathin 2D metal–organic framework nanosheets. Adv. Mater. 27 (45), 7372–7378.

Zhao, W., Peng, J., Wang, W., Liu, S., Zhao, Q., Huang, W., 2018c. Ultrathin two-dimensional metal–organic framework nanosheets for functional electronic devices. Coord. Chem. Rev. 377, 44–63.

Zhao, X., Wang, Y., Li, D.-S., Bu, X., Feng, P., 2018d. Metal–organic frameworks for separation. Adv. Mater. 30 (37), 1705189.

Zhao, Y., Jiang, L., Shangguan, L., Mi, L., Liu, A., Liu, S., 2018e. Synthesis of porphyrin-based two-dimensional metal–organic framework nanodisk with small size and few layers. J. Mater. Chem. 6 (6), 2828–2833.

Zheng, H.-Q., Liu, C.-Y., Zeng, X.-Y., Chen, J., Lü, J., Lin, R.-G., Cao, R., Lin, Z.-J., Su, J.-W., 2018. MOF-808: a metal–organic framework with intrinsic peroxidase-like catalytic activity at neutral pH for colorimetric biosensing. Inorg. Chem. 57 (15), 9096–9104.

Zhou, J., Li, M., Hou, Y., Luo, Z., Chen, Q., Cao, H., Huo, R., Xue, C., Sutrisno, L., Hao, L., Cao, Y., Ran, H., Lu, L., Li, K., Cai, K., 2018a. Engineering of a nanosized biocatalyst for combined tumor starvation and low-temperature photothermal therapy. ACS Nano 12 (3), 2858–2872.

Zhou, J., Tian, G., Zeng, L., Song, X., Bian, X.-w., 2018b. Nanoscaled metal-organic frameworks for biosensing, imaging, and cancer therapy. Adv. Healthc. Mater. 7 (10), 1800022.

Zhou, J., Tian, G., Zeng, L., Song, X., Bian, X.w., 2018c. Nanoscaled metal-organic frameworks for biosensing, imaging, and cancer therapy. Adv. Healthc. Mater. 7 (10) 1800022.

Zhu, D., Guo, C., Liu, J., Wang, L., Du, Y., Qiao, S.-Z., 2017. Two-dimensional metal–organic frameworks with high oxidation states for efficient electrocatalytic urea oxidation. Chem. Commun. 53 (79), 10906–10909.

Zhu, P., Chen, Y., Shi, J., 2018. Nanoenzyme-augmented cancer sonodynamic therapy by catalytic tumor oxygenation. ACS Nano 12 (4), 3780–3795.

Ziyatdinova, G., Kozlova, E., Budnikov, H., 2018. Selective electrochemical sensor based on the electropolymerized p-coumaric acid for the direct determination of l-cysteine. Electrochim. Acta 270, 369–377.

Zong, C., Xu, M., Xu, L.-J., Wei, T., Ma, X., Zheng, X.-S., Hu, R., Ren, B., 2018. Surface-enhanced Raman spectroscopy for bioanalysis: reliability and challenges. Chem. Rev. 118 (10), 4946–4980.